Activating *PIK3CD* mutations impair human cytotoxic lymphocyte differentiation and function and EBV immunity

Emily S.J. Edwards PhD[ab*]. Julia Bier MSc[ab]. Theresa S. Cole MD, PhD[c]. Melanie Wong MBBS, PhD, FRACP, FRCPA[de]. Peter Hsu FRACP, PhD[deg]. Lucinda J. Berglund MBBS, PhD[efh]. Kaan Boztug MD[i]. Anthony Lau BSc[ab]. Emma Gostick BSc[j]. David A. Price MRCP, D Phil[jk]. Michael O'Sullivan MBBS[l]. Isabelle Meyts MD, PhD[mn]. Sharon Choo MBBS, FRACP, FRCPA[co]. Paul Gray FRACP[ep]. Steven M. Holland MD[q]. Elissa K. Deenick PhD[abe]. Gulbu Uzel MD[q]. Stuart G.Tangye PhD[abe].

[a] Immunology Division, Garvan Institute of Medical Research, Australia
[b] St Vincent's Clinical School, Faculty of Medicine, University of New South Wales Sydney, Australia
[c] Department of Allergy and Immunology, Royal Children's Hospital, Melbourne, Australia
[o] Immunology Laboratory, Laboratory Services, Royal Children's Hospital, Melbourne, Australia
[d] Children's Hospital at Westmead, Westmead, Australia
[e] CIRCA (Clinical Immunogenomics Consortia Australia), Sydney, Australia
[f] Immunopathology Department, Westmead Hospital, Westmead, Australia
[g] Discipline of Child and Adolescent Health, Faculty of Medicine, University of Sydney, Australia
[h] Faculty of Medicine, University of Sydney, Sydney, Australia
[I] CeMM Research Center for Molecular Medicine of the Austrian Academy of Sciences, Vienna, St Anna Children's Hospital and Children's Cancer Research Institute, Department of Paediatrics and Adolescent Medicine, Medical University of Vienna, and Ludwig Boltzmann Institute for Rare and Undiagnosed Diseases, Austria
[j] Division of Infection and Immunity, Cardiff University School of Medicine, Cardiff, United Kingdom
[k] Vaccine Research Center, National Institute of Allergy and Infectious Disease, National Institutes of Health, Bethesda
[l] Perth Children's Hospital, Perth, Australia
[m] Department of Pediatrics, University Hospital Leuven, Leuven, Belgium
[n] Department of Microbiology and Immunology, Childhood Immunology, KU Leuven, Belgium
[p] University of New South Wales School of Women's and Children's Health, Randwick, Australia
[q] Laboratory of Clinical Immunology and Microbiology, National Institute of Allergy and Infectious Diseases, National Institutes of Health, Bethesda, Md

Background

Germline gain-of function (GOF) mutations in *PIK3CD*, encoding the catalytic p110δ subunit of phosphoinositide 3-kinase (PI3K), result in hyperactivation of the PI3K–AKT–mechanistic target of rapamycin pathway and underlie a novel inborn error of immunity. Affected subjects exhibit perturbed humoral and cellular immunity, manifesting as recurrent infections, autoimmunity, hepatosplenomegaly, uncontrolled EBV and/or cytomegalo-virus infection, and increased incidence of B-cell lymphoproliferation, lymphoma, or both. Mechanisms underlying disease pathogenesis remain unknown.

Objective

Understanding the cellular and molecular mechanisms underpinning inefficient surveillance of EBV-infected B cells is required to understand disease in patients with *PIK3CD* GOF mutations, identify key molecules required for cell-mediated immunity against EBV, and develop immunotherapeutic interventions for the treatment of this and other EBV-opathies.

Methods

We studied the consequences of *PIK3CD* GOF mutations on the generation, differentiation, and function of $CD8^+$ T cells and natural killer (NK) cells, which are implicated in host defense against infection with herpes viruses, including EBV.

Results

PIK3CD GOF total and EBV-specific CD8$^+$ T cells were skewed toward an effector phenotype, with exaggerated expression of markers associated with premature immunosenescence/exhaustion and increased susceptibility to reactivation-induced cell death. These findings were recapitulated in a novel mouse model of PI3K GOF mutations. NK cells in patients with *PIK3CD* GOF mutations also exhibited perturbed expression of differentiation-associated molecules. Both CD8$^+$ T and NK cells had reduced capacity to kill EBV-infected B cells. *PIK3CD* GOF B cells had increased expression of CD48, programmed death ligand 1/2, and CD70.

Conclusions

PIK3CD GOF mutations aberrantly induce exhaustion, senescence, or both and impair cytotoxicity of CD8$^+$ T and NK cells. These defects might contribute to clinical features of affected subjects, such as impaired immunity to herpesviruses and tumor surveillance.

Phosphoinositide 3-kinase (PI3K) signaling is pivotal in regulating many cellular processes involved in lymphocyte biology, including differentiation, proliferation, apoptosis, metabolism, and effector function.[1] In human subjects *PIK3CD* encodes the p110δ isoform of the catalytic subunit of PI3K. p110δ is expressed predominantly in hematopoietic cells and forms a heterodimer with the p85α regulatory subunit.[2, 3] Ligation of molecules linked to tyrosine kinase activity, including CD8, T-cell receptor (TCR), and CD28, potentiates recruitment and activation of p110δ, resulting in activation of downstream effector molecules. PI3K activation is regulated by phosphatase and tensin homolog and SH2 domain-containing inositol 5′-phosphatase, which dephosphorylate substrates of p110δ.[4, 5]

CD8$^+$ T cells require changes in metabolism as a means of regulating their differentiation, proliferative capacity, effector function, and memory generation.[6, 7] Mechanistic target of rapamycin (mTOR) is a metabolic checkpoint kinase activated by PI3K and plays a key role in regulating glycolysis.[8, 9] After encounter with specific antigen, naive T cells can differentiate into effector cells, culminating in activation of the PI3K-AKT-mTOR pathway and a metabolic shift toward glycolysis. Previous studies demonstrated that mice expressing catalytically inactive p110δ exhibit defects in TCR signaling.[10] Furthermore, CD8$^+$ T-cell responses in these mice to *Listeria monocytogenes* infection[11] and their migratory capacity were impaired.[12] PI3K-AKT signaling also modulates the differentiation, development, and activation of NK cells. In p110δ-deficient mice, as well as in PI3K inhibitor–treated human cells, attenuated p110δ signaling causes decreased NK cell numbers, terminal differentiation, cytokine production, cytotoxicity, and migration.[13, 14, 15]

The importance of the PI3K-AKT pathway in modulating signals in lymphocytes is highlighted by various pathologic conditions that result from aberrant signaling through this pathway.[16, 17] To date, more than 100 subjects with heterozygous mutations in *PIK3CD*have been described, with most having the recurrent E1021K mutation in the catalytic domain of p110δ. These mutations cause constitutive activation of the PI3K-AKT-mTOR pathway and are thus gain-of-function (GOF) mutations.[18, 19] Affected subjects present with clinical features, including recurrent respiratory tract infections, lymphadenopathy, impaired humoral immune responses, increased susceptibility to EBV and/or cytomegalovirus (CMV), autoimmunity, and increased incidence of B-celllymphoproliferation, lymphoma, or both.[18, 19, 20, 21] *PIK3CD* GOF mutations decrease total CD4$^+$ T-cell frequencies and numbers of naive CD4$^+$ and CD8$^+$ T cells, with concomitant increases in numbers of effector memory CD8$^+$ T cells.[17, 18, 19, 20, 21, 22] Numbers of natural killer (NK) cells are also reduced in some subjects.[17, 18, 19, 20]

To understand immune dysregulation and increased susceptibility to EBV-induced disease in patients with *PIK3CD* GOF mutations, we performed in-depth analysis of the differentiation, activation, and function of their CD8$^+$ T cells and NK cells. Activating mutations in *PIK3CD*cause a premature immunosenescent/ exhaustion-

type phenotype of $CD8^+$ T cells and altered differentiation of NK cells, resulting in impaired cytotoxicity of both cell subsets against EBV-infected B cells. These findings provide insight into some of the clinical features of *PIK3CD* GOF mutations, including impaired control of EBV and susceptibility to B-cell lymphoma.

METHODS

Clinical evaluation

PBMCs were isolated from healthy anonymous blood donors obtained from the Australian Red Cross Service and patients with *PIK3CD* GOF mutations (Table I).[19, 23, 24] Viral infection history of healthy donors was unknown. Whole blood was collected from Australian-based patients and sent immediately to the Garvan Institute of Medical Research. PBMCs were isolated and either analyzed fresh or cryopreserved and stored in liquid nitrogen until use. For patients outside of Australia, PBMCs were isolated and cryopreserved as single-cell suspensions as above, shipped to the Garvan Institute on dry ice, and then stored in liquid nitrogen until use. This study was approved by institutional human research ethics committees at the relevant institutions.

T, B, and NK cell phenotyping

PBMCs from healthy control subjects and patients with *PIK3CD* GOF mutations were labeled with mAbs against CD3, CD4, CD8, CD20, and CD56. $CD8^+$ T-cell subsets were defined as naive T (T_N; $CD8^+CD4^-CCR7^+CD45RA^+$), central memory T (T_{CM}; $CD8^+CD4^-CCR7^+CD45RA^-$), effector memory T (T_{EM}; $CD8^+CD4^-CCR7^-CD45RA^-$), and terminally differentiated effector memory T expressing CD45RA (T_{EMRA}; $CD8^+CD4^-CCR7^-CD45RA^+$) cells. B cells were defined as $CD3^-CD20^+$ cells, and NK cells were defined as $CD3^-CD56^+$ cells. Typing for HLA-A, HLA-B, and HLA-C was performed by the Australian Red Cross Service. PBMCs from patients with *PIK3CD* GOF mutations and healthy control subjects were stained with 20 μg/mL EBV-specific tetramers (Table E1) at 37°C for 20 minutes.[25]

For phenotyping, cells were further stained with cell-surface and intracellular antibodies (Table E2). For Vβ repertoire staining, PBMCs were stained further with the IOTest Beta Mark kit (Beckman Coulter, Brea, Calif), according to the manufacturer's instructions. Data were acquired on an LSRII SORP (Becton Dickinson, Mountain View, Calif) and analyzed with FlowJo software (TreeStar, Ashland, Ore). Based on Boolean gating analysis, coexpression of CD57, KLRG1, and programmed cell death protein 1 (PD-1) was determined by using Prism 7 software (GraphPad Software, La Jolla, Calif).

Analysis of CD8+ T-cell functional capacity in vitro

Sorted T_{EM} ($CD8^+CD4^-CCR7^-CD45RA^-$) and T_{EMRA}($CD8^+CD4^-CCR7^-CD45RA^+$) $CD8^+$ T cells were cultured in 96-well round-bottom plates (3×10^4 cells/well) with T-cell expansion and activation (TAE; anti-CD3, anti-CD28, and anti-CD2 mAb) beads (Miltenyi Biotech, Bergisch Gladbach, Germany). After 5 days, supernatants were harvested and assayed for production of IFN-γ, TNF-α, IL-2, granzyme A, and granzyme B by using a cytometric bead array (Becton Dickinson, Franklin Lakes, NJ). For cytokineexpression, activated $CD8^+$ T cells were restimulated with phorbol 12-myristate 13-acetate (PMA; 100 ng/mL)/ ionomycin (750 ng/mL) for 6 hours, with Brefeldin A (10 μg/ml; Sigma-Aldrich, St Louis, Mo), monensin (2 μmol/L; eBioscience, Waltham, Mass), and anti-CD107a (Becton Dickinson, Franklin Lakes, NJ) added after 2 hours. Cells were fixed and stained for expression of IFN-γ, TNF-α, IL-2 (BD Horizon, Mountain View, Calif), granzyme B (BD PharMingen, San Jose, Calif), and perforin (BioLegend, San Diego, Calif). Samples were acquired on an LSRII SORP (Becton Dickinson) and analyzed with FlowJo software.

Cell proliferation

PBMCs were labeled with carboxyfluorescein succinimidyl ester (2.5 μmol/L; eBioscience, Carlsbad, Calif) and then cultured at 1.2×10^5 cells per well with TAE beads (1 bead per 2 cells) with or without 50 U/mL IL-2 (Millipore, Darmstadt, Germany) or 5 μg/mL PHA (Sigma-Aldrich) plus 50 U/mL IL-2 for 3 or 5 days. Cells were stained with Zombie Aqua Fixable Dye (BioLegend), fixed, and run on the LSR II Fortessa (Becton Dickinson). Data were analyzed with FlowJo software.

Cytotoxic T-cell and NK cell killing assays (including T-cell line and NK lymphokine-activated killer cell generation)

EBV-specific T-cell lines were generated from patient or control PBMCs, as previously described.[26, 27] Cytotoxicity and intracellular cytokine stimulation assays against autologous lymphoblastoid cell lines (LCLs) were performed after the third restimulation cycle. Sorted NK cells ($CD3^-CD56^+$) were stimulated with 100 U/mL IL-2 in RPMI 1640/20% FCS, and cytotoxicity against autologous LCLs was assessed on day 10.

NK and cytotoxic T-lymphocyte cytotoxicity was assessed by using a CytoTox 96 Non-Radioactive Cytotoxicity Assay (Promega, Madison, Wis), as previously described.[19] Briefly, 10,000 target cells (LCLs) were plated at various effector/target ratios with NK cells (5:1 or 10:1) or cytotoxic T lymphocytes (2.5:1, 5:1, 7.5:1, or 10:1) in U-bottom plates at 37°C. After 4 hours, supernatants were collected and assayed to determine the amount of lactate dehydrogenase released on cell lysis by using colorimetry. Percentage cytotoxicity was determined by using the following equation from the manufacturer's instructions:

% Cytotoxicity = Experimental value − (Corrected effector spontaneous + Corrected target spontaneous) × 100/

Corrected target maximum − Corrected target spontaneous.

Sorting and culture of B cells

Total B cells ($CD20^+$, >98% purity) were sorted from PBMCs from healthy control subjects or patients with *PIK3CD* GOF mutations by using a FACSAria III (Becton Dickinson). B cells or LCLs were seeded at 30,000 cells/well in a U-bottom plate and cultured in RPMI 1640/10% FCS or stimulated with 2.5 μg/mL CD40 ligand (R&D Systems, Minneapolis, Minn) with or without 2.5 μg/mL anti-immunoglobulin. On day 3, cells were stained with mAbs to anti-CD48, HLA-DR(BD PharMingen), CD95 (BD Horizon), CD70, HLA-ABC, programmed death ligand (PD-L) 1−PE or PD-L2 (eBioscience) and run on an LSRII Fortessa (Becton Dickinson).

Restimulation-induced cell death, RNA extraction, and quantitative PCR analysis

Restimulation-induced cell death (RICD) was determined, as previously described.[28, 29] T_{EM} and T_{EMRA} $CD8^+$ T cells were sorted (>98% purity) on a FACSAria III and cultured with TAE beads. On day 3, 100 U/mL IL-2 was added, and cells were maintained for 10 days, replacing IL-2 every 3 days. On day 13, cells were counted and seeded with medium alone or medium with 1 μg/mL plate-bound α-CD3 mAb (UCHT1; Biogems, Westlake Village, Calif) plus 100 U/mL I-L2 or 20 ng/mL α-CD95 mAb (APO-1-3, Enzo Lifesciences, Farmington, NY) plus 100 U/mL IL-2. Cells were then cultured overnight and stained with Zombie Live/Dead Fixable Aqua to determine the frequency of dead cells.[28, 29] To assess Fas ligand *(FASLG)* mRNA expression, cells were stimulated for 4 hours with anti-CD3 plus 100 U/mL IL-2, and total RNA was then extracted. Quantitative polymerase chain reaction was performed by using the Light Cycler 480 Probe Master Mix and System (Roche, Mannheim, Germany). *FASLG*(forward: 5′-CAGAAGGAGCTGGCAGAACT-3′; reverse: 5′-TGGCCTATTTGCTTCTCCAA-3′) and glyceraldehyde-3-phosphate dehydrogenase *(GAPDH)* primers (forward: 5′-CTCTGCTCCTCCTGTTCGAC-3′; reverse: 5′-ACGACCAAATCCGTTGACTC-3′) were obtained from Integrated DNA Technologies (Coralville, Iowa). Expression of Fas ligand was determined relative to expression of *GAPDH*.

Murine flow cytometric phenotyping

Spleens of wild-type or *Pik3cd*^{E1020K} GOF mice were harvested, prepared, and stained for flow cytometry, as previously described,[30] by using the mAbs listed in Table E3 Data were acquired on either the LSRII SORP or LSR Fortessa (Becton Dickinson) and analyzed with FlowJo software. All data are representative of 2 or more experiments, as indicated. All animal studies were approved by the St Vincent's Animal Ethics Committee.

Murine in vitro cultures

Sorted *Pik3cd*^{E1020K} GOF or wild-type naive CD8$^+$ T cells were cultured in flat-bottom 96-well plates coated with anti-CD3 (4 μg/mL; BioLegend) in RPMI 1640 (Life Technologies, Grand Island, NY) supplemented with 10% FCS (Life Technologies) at 0.5×10^6 cells/mL. After 4 days, cells were stimulated with PMA (50 ng/mL) and ionomycin (375 ng/mL) for 6 hours. Brefeldin A (10 μg/mL) was added to each well at 2 hours of culture. Cells were then harvested, washed, and stained with Zombie Aqua Viability Dye (BioLegend). CD8$^+$ T cells were fixed, permeabilized, and stained with mAbs to anti–TNF-α and anti–IFN-γ and analyzed by using flow cytometry.

Statistical analysis

For single comparisons of independent groups, a Mann-Whitney test was performed. For multiple comparisons, 2-way ANOVA or multiple *t* tests were applied as follows. Analyses were performed with GraphPad Prism software.

RESULTS

Patients with *PIK3CD* GOF mutations present with features of EBV-associated disease

In this study we investigated 39 patients from 28 families (18 male and 21 female patients) with activating mutations in *PIK3CD*. The E1021K mutation was found in 28 of 39 patients.[19, 31] The other mutations identified in patients in this study (ie, G124D, N334K, E525K, and E1025G) have been reported previously and confirmed to be GOF mutations.[19, 23, 24] Patients' ages ranged from 4.5 to 67 years (mean, 20.1 years), with patients originating from a variety of ethnicities (Table I). As control subjects, we analysed PBMCs from 38 healthy donors whose ages ranged from 10 to 71 years (mean, 38.0 years). Overall, 19 subjects were confirmed to be EBV$^+$ by using PCR, whereas 6 subjects were CMV$^+$ (Table I). The 6 CMV$^+$ subjects were also EBV$^+$. Four patients had B-celllymphoma (2 EBV$^+$ subjects, Table I). The incidences of EBV/CMV infection/viremia and B-cell malignancy in this cohort are comparable with that reported previously.[20]

CD8$^+$ T cells are increased and are enriched as effector memory cells in patients with *PIK3CD* GOF mutations

To investigate the effect of *PIK3CD* GOF mutations on cytotoxic lymphocytes, we first determined proportions of peripheral blood T-cell populations and subsets. Compared with healthy control subjects, patients with *PIK3CD* GOF mutations had increased frequencies of CD8$^+$ T cells and a corresponding decrease in numbers of CD4$^+$ T cells, thereby yielding a significantly inverted CD4/CD8 ratio (Fig 1, *A-C*). The CD4/CD8 ratio tends to increase with age, being approximately 1.5 to 2.0 for 20-year-olds and gradually increasing to 2.5 to 3.0 by 80 years of age.[32] Therefore one explanation for the decreased CD4/CD8 ratio in our cohort could be that approximately 60% of patients in our study were aged 20 years or less (Table I). To formally test this, we determined the CD4/CD8 ratio for a range of healthy donors and patients with *PIK3CD* GOF mutations as a function of age. As shown in Fig 1, *D*, a decreased CD4/CD8 ratio was observed consistently for all age groups of patients with *PIK3CD* GOF mutations compared with control subjects, establishing that this parameter was not influenced by an enrichment of younger patients in our study cohort versus the healthy control subjects.

CD8$^+$ T cells can be divided into naive and memory subsets based on differential expression of CCR7 and CD45RA.[33] A population of T cells, termed stem cell memory-like T (T_{SCM}) cells, with self-renewal properties

and the capacity to form effector memory cells on antigen encounter, has also been identified. Like naive cells, T_{SCM} cells are also $CCR7^+CD45RA^+$. However, T_{SCM}cells can be distinguished from naive cells by their expression of CD95.[34] Thus in our analyses we refer to $CD45RA^+CCR7^+CD8^+$ T cells as T_N/T_{SCM} cells. Applying this analysis revealed an expansion of T_{EM} cells ($CCR7^-CD45RA^-$) with a corresponding reduction in T_N/T_{SCM} (mostly naive) cells in patients with *PIK3CD* GOF mutations compared with healthy control subjects. The proportions of T_{CM} ($CCR7^+CD45RA^-$) cell and T_{EMRA} ($CCR7^-CD45RA^+$) cell subsets in the patients were in the normal range (Fig 1, *E* and *F*). Similarly, *PIK3CD* GOF mutations resulted in fewer T_N $CD4^+$ cells but significantly increased proportions of T_{CM} $CD4^+$ cells (not shown).

$CD8^+$ T cells from patients with *PIK3CD* GOF mutations are skewed toward a phenotype consistent with functional exhaustion and senescence

CD57 expression can delineate populations of senescent $CD8^+$ T and NK cells.[35, 36] Previous reports suggested $CD8^+$ T cells in patients with *PIK3CD*GOF mutations are predominantly of a senescent phenotype, as evidenced by increased proportions of $CD57^+$ cells.[19, 20, 21, 22] After chronic infection and therefore constant antigen stimulation, $CD8^+$ T cells can also adopt a state of exhaustion, which is defined as the progressive and hierarchical loss of effector function, a concomitant acquisition of inhibitory or regulatory surface receptors, and alterations in cytokine, chemotactic, survival, and metabolic signaling pathways.[37, 38]

For these reasons, we first performed comprehensive phenotypic analysis of total $CD8^+$ T cells in patients with *PIK3CD* GOF mutations and control subjects. To achieve this, we quantified expression of surface molecules associated with $CD8^+$ T-cell activation (CD38, HLA class I, and HLA class II),39, 40differentiation, exhaustion (CD95, CD160, KLRG1, and PD-1),[38, 41, 42, 43, 44, 45] and senescence (CD57).[35, 36] The proportions of total *PIK3CD* GOF $CD8^+$T cells that expressed these molecules were significantly increased compared with those in control subjects (Fig 2).

Next, we determined expression of these molecules on $CD8^+$ T cells at distinct stages of differentiation. CD160 expression did not differ among the $CD8^+$ T-cell subsets examined, whereas expression of CD95 and KLRG1 was significantly increased on naive and T_{CM} cells, respectively. In contrast, the other molecules examined were detected on significantly greater proportions of T_N, T_{CM}, T_{EM}, and T_{EMRA} $CD8^+$ T-cell subsets (Fig 2). Thus the increased expression of these markers of differentiation on $CD8^+$ T cells did not simply reflect accumulation of T_{EM} cells (Fig 1, *E*). Rather, these data reveal the general senescent and/or exhausted-type state of most subsets of $CD8^+$ T cells in patients with *PIK3CD*GOF mutations, which is consistent with analyses of much smaller cohorts of patients with *PIK3CD* GOF mutations.[19, 22]

We also examined expression of 2B4 (CD244) and NKG2D (CD314), molecules implicated in $CD8^+$ T and NK cell–mediated control of EBV-infected B cells.[26, 46, 47] 2B4 is also a marker of $CD8^+$ T-cell exhaustion.[37, 38] 2B4 was increased on total T cells because of upregulation on T_N, T_{CM}, and T_{EM} $CD8^+$ cells (Fig 2, *B*). In contrast, relative NKG2D expression was only modestly increased on naive $CD8^+$ T cells (Fig 2, *J*).

In patients with HIV or chronic hepatitis B or C virus infection, coexpression of a suite of regulatory molecules on $CD8^+$ T cells correlates with exhaustion and impaired effector function of these cells.[38, 41, 44, 48] Therefore we investigated coexpression of PD-1, KLRG1, and CD57 on $CD8^+$ T cells from patients with *PIK3CD* GOF mutations and control subjects. Strikingly, a larger frequency of *PIK3CD* GOF $CD8^+$ T cells coexpressed CD57, 2B4, and KLRG1 compared with control subjects in which few coexpressed these 3 receptors (Fig 2, *K*). Importantly, the "exhausted-type" phenotype of *PIK3CD* GOF $CD8^+$ T cells appeared to result directly from the genetic mutation rather than pathogen or chronic viral infection because similar phenotypic characteristics of $CD8^+$ T cells were observed in patients who were EBV naive or who had mild or chronic EBV viremia.

We also analyzed the Vβ repertoire of the different subsets of $CD8^+$ T cells by determining expression of individual TCR Vβ chains through flow cytometry. TCR Vβ repertoires of patients with *PIK3CD* GOF mutations and control subjects were similar. Differences in the most predominant Vβ chain use between subjects likely

reflects the diversity of pathogens encountered and the immunogenicity of the antigenic peptides they encode (Fig E1). Collectively, our results indicate that *PIK3CD* GOF mutations result in sustained and exaggerated activation of polyclonal $CD8^+$ T cells, yielding prematurely immunosenescent and exhausted-type $CD8^+$ T cells.

EBV-specific $CD8^+$ T cells are skewed toward a T_{EM} phenotype in patients with *PIK3CD* GOF mutations

Next, we investigated whether generation of EBV-specific $CD8^+$ T cells was affected by *PIK3CD* GOF mutations. In 14 subjects in whom HLA class I typing was available, PBMCs from patients and HLA-matched control subjects were stained *ex vivo* with MHC class I peptide tetramers and dextramers to identify EBV-specific T cells (Table E1). Comparable frequencies of EBV-specific $CD8^+$ T cells were detected in patients with *PIK3CD* GOF mutations and healthy HLA-matched control subjects (Fig 3, *A*). In healthy donors most EBV-specific $CD8^+$ T cells have a T_{CM} or T_{EM} phenotype (Fig 3, *B*).[49, 50] In contrast, most EBV-specific $CD8^+$ T cells in patients with *PIK3CD* GOF mutations exhibited a T_{EM} phenotype (Fig 3*B*). Similar to total polyclonal $CD8^+$ T cells, expression of CD57, KLRG1, CD160, CD95, CD38, PD-1, 2B4, and NKG2D was increased significantly on EBV-specific $CD8^+$ T cells from patients with *PIK3CD* GOF mutations compared with healthy control subjects. Moreover, the vast majority of EBV-specific T cells in patients with *PIK3CD* GOF mutations coexpressed the regulatory receptors 2B4, KLRG1, and/or CD57, whereas in healthy control subjects more than 60% of EBV-specific T cells lacked expression of these markers. These data suggest that, akin to total *PIK3CD* GOF $CD8^+$ T cells and $CD8^+$ T cells specific for HIV, hepatitis B and hepatitis C virus,[38, 41, 48, 51] EBV-specific *PIK3CD* GOF T cells acquire a phenotype consistent with premature senescence, exhaustion, or both and impaired effector function.

***PIK3CD* GOF mutations alter the functionality of $CD8^+$ T cells**

To determine the effect of *PIK3CD* GOF mutations on $CD8^+$ T-cell function, we first assessed proliferation. Cell division, as measured based on carboxyfluorescein succinimidyl ester dilution, after *in vitro* stimulation with PHA/IL-2 or mAbs specific for CD2, CD3, and CD28 with or without IL-2 was unaffected by *PIK3CD* GOF mutations (Fig 4, *A* and *B*). Although these data appear to contrast previous studies that observed decreased proliferation of *PIK3CD* GOF T cells in response to CD3/CD28 stimulation, Lucas et al[19]reported that inclusion of anti-CD2 mAbs could overcome defective proliferation of *PIK3CD* GOF T cells. Thus our data are concordant with previously published findings.

Expression of granzymes A, B, and K and perforin, components of the cytolytic machinery, was increased in total and EBV-specific (Fig 4, *E* and *F*, and Fig E2, *B*) *PIK3CD* GOF $CD8^+$ T cells. Proportions of total *PIK3CD* GOF $CD8^+$ T cells expressing IFN-γ or CD107a were increased (Fig 4, *G* and *H*) and those expressing IL-2 were decreased (Fig 4, *I*) on *ex vivo* stimulation with PMA/ionomycin.

To ascertain whether T_{EM} cell expansion was responsible for the observed $CD8^+$T-cell dysfunction in patients with *PIK3CD* GOF mutations, we sorted T_{EM} and T_{EMRA} subsets, stimulated them with anti-CD2/CD3/CD28 mAbs, and measured cytokine expression and degranulation. A higher proportion of T_{EM} cells from patients with *PIK3CD* GOF mutations expressed IFN-γ and CD107a compared with those from control subjects; however, a reduced proportion of these cells expressed IL-2 (Fig E2, *C*). Expression of granzyme B and perforin were not significantly different in activated T_{EM} cells from patients and control subjects (Fig E2, *C*). In contrast, the frequency of IFN-γ–expressing T_{EMRA} cells was reduced by *PIK3CD* GOF mutations (Fig E2, *D*). There were trends for greater expression of CD107a, granzyme B, and IL-2 in T_{EMRA} cells from patients with *PIK3CD* GOF mutations compared with control subjects, but these differences did not reach statistical significance. Our flow cytometric analysis of $CD8^+$ T-cell subsets was confirmed when secretion of effector molecules was determined, showing that T_{EM} cells from patients with *PIK3CD* GOF mutations secreted larger quantities of cytokines and cytolytic molecules compared with healthy subjects (Fig E2, *C*). The phenotypic differences observed in total $CD8^+$ T cells was largely observed when examining the T_{EM} compartment, such as significant increases in the expression of CD57, PD-1, CD38, 2B4, and HLA class I and II.

Next, we addressed the effect of *PIK3CD* GOF mutations on $CD8^+$ T cell–mediated immunity to EBV. To test this, we generated $CD8^+$ T-cell lines against autologous EBV-transformed B-LCLs. EBV-specific $CD8^+$ T-cell lines from patients with *PIK3CD* GOF mutations exhibited reduced cytotoxicity toward autologous LCLs at effector/target ratios of between 5:1 and 10:1 (Fig 4, *J* and *K*). Thus *PIK3CD* GOF $CD8^+$ T cells exhibit dysregulated cytokine expression and defective cytotoxic function against EBV-LCLs.

Increased RICD of PIK3CD GOF $CD8^+$ T cells

RICD is an apoptotic mechanism used to limit effector T-cell expansion, thereby restricting the risk of nonspecific damage to the host. Defects in this process have been proposed to contribute to host tissue damage and unrestrained T-cell accumulation in patients with X-linked lymphoproliferative disease because of SLAM-associated protein deficiency.[29] RICD is triggered in effector cells by using TCR ligation, which upregulates proapoptotic Fas ligand to induce autocrine cell death. Thus Fas ligand expression correlates with RICD susceptibility.[28, 29] To ascertain whether RICD was affected, T_{EM} and T_{EMRA}cells were sorted from patients with *PIK3CD* GOF mutations and healthy control subjects stimulated with CD2, CD3, and CD28 mAbs, with IL-2 being added on day 3. Ten days after addition of IL-2, cells were stimulated with either α-CD3 mAb to induce RICD or α-CD95 mAb to determine the sensitivity to CD95-mediated apoptosis. Increased RICD was observed in T_{EM}, but not T_{EMRA}, cells from patients with *PIK3CD* GOF mutations compared with corresponding cells from control subjects (Fig 4, *K*). This correlated with greatly increased expression of *FASLG* in cells from patients with *PIK3CD* GOF T_{EM} mutations relative to control T_{EM} cells (Fig 4, *L*). There was also greater death of T_{EM}, but not T_{EMRA}, cells induced by a suboptimal concentration of anti-CD95 mAbs (Fig 4, *M*). Collectively, these data indicate that *PIK3CD* GOF mutations render T_{EM}cells more susceptible to apoptosis induced by RICD or engagement of CD95.

***PIK3CD* GOF mutations dysregulate NK cell differentiation and function**

NK cells also play key roles in host defense against viral infection, including herpesviruses; for instance, NK cells control EBV in patients with infectious mononucleosis.[52, 53] For this reason, we examined the NK cell compartment of patients with *PIK3CD* GOF mutations. NK cell frequencies as a percentage of peripheral blood lymphocytes (Fig 5, *A*) and proportions of $CD56^{bright}$ and $CD56^{dim}$ subsets were unaltered by *PIK3CD* GOF mutations. However, further analysis revealed that expression of CD57, CD158a/g/h, CD16, granzyme B, perforin, and HLA class I was significantly increased on both $CD56^{bright}$ and $CD56^{dim}$ NK cell subsets from patients with *PIK3CD* GOF mutations (Fig 5, *A*-*J*). NKG2A was also upregulated on $CD56^{dim}$ and KLRG1 was increased on $CD56^{bright}$*PIK3CD* GOF NK cells (Fig 5, *D* and *F*). In contrast, *PIK3CD* GOF had no effect on 2B4 or NKG2D expression.

Lymphokine-activated killer cells were generated from patients and control subjects and then stimulated with autologous EBV-LCLs to determine whether NK cell cytotoxic function was affected by *PIK3CD* GOF mutations and altered effector phenotype. *PIK3CD* GOF lymphokine-activated killer cells exhibit decreased cytotoxicity in response to autologous LCLs (Fig 5, *K* and *L*). Thus NK cells in patients with *PIK3CD* GOF mutations exhibit dysregulated expression of key regulatory molecules and reduced cytotoxic function.

Altered expression of regulatory ligands on B cells in patients with *PIK3CD* GOF mutations

To extend our analysis of defects in pathways controlling cytotoxicity of NK cells and $CD8^+$ T cells, we determined expression of ligands of 2B4 (CD48), PD-1 (PD-L1 and PD-L2), and CD27 (CD70), which have been shown to be dysregulated on B-cell lymphomas and/or EBV-infected B cells,[47, 54, 55] on B cells from patients with *PIK3CD* GOF B mutations. We analyzed primary B cells and LCLs before and after stimulation with CD40 ligand/anti-immunoglobulin. CD48 and CD70 were upregulated on *PIK3CD* GOF B cells relative to control B cells *ex vivo* (Fig 6, *A*). On stimulation, primary B cells upregulated PD-L1, PD-L2, and CD70 (Fig 6, *A*), with significantly higher expression on activated

Heightened expression of CD48, PD-L1, PD-L2, and CD70 was also observed for unstimulated LCLs from patients with *PIK3CD* GOF mutations compared with control LCLs, with further upregulation on *PIK3CD* GOF

LCLs after activation CD40 ligand/anti-immunoglobulin (Fig 6, *B*). Similar results were obtained when we assessed expression of HLA class I, HLA class II, and CD95 on resting and activated primary B cells and LCLs from healthy control subjects and patients with *PIK3CD* GOF mutations (Fig E3, *A* and *B)*. Taken together, these findings establish that *PIK3CD* GOF B cells express increased levels of ligands that regulate cytotoxicity of $CD8^+$ T cells and NK cells.

Mice bearing a PI3K p110δ GOF mutation phenocopy defects in human *PIK3CD*GOF $CD8^+$ T cells

Many patients with *PIK3CD* GOF mutations have chronic or severe herpesvirus infections.[19, 20] Thus to confirm that the changes we observed in $CD8^+$ T-cell differentiation were cell intrinsic and not secondary to pathogen infection, we generated a mouse model. We used CRISPR/Cas9-mediated gene editing to introduce a heterozygous glutamic acid (E) to lysine (K) substitution at amino acid number 1020 of the murine PI3K p110δ protein. This corresponds to the common E1021K mutation found in approximately 75% of patients with *PIK3CD*GOF mutations. The $CD8^+$ T-cell compartment in the spleens of young (8-12 weeks) and aged (33 weeks) *Pik3cd*^{E1020K} mice recapitulated the phenotype observed in patients with *PIK3CD* GOF mutations. Thus there were significantly reduced proportions of naive and corresponding increased proportions of central memory and effector memory $CD8^+$ T cells in *Pik3cd*^{E1020K} mice compared with littermate control mice (Fig 7, *A-C*). These differences were exacerbated with age and also evident in blood (Fig 7, *A-C*). Functional analysis demonstrated increased production of IFN-γ and TNF-α by *in vitro* cultured naïve *Pik3cd*^{E1020K}$CD8^+$ T cells compared with control cells (Fig 7, *D*). This initial analysis of our novel *in vivo* model of human disease caused by PI3K p110δ GOF has established that dysregulation of $CD8^+$ T-cell responses occurs independently of infection or immunization.

DISCUSSION

Activating mutations in *PIK3CD* underlie a novel disease of immune dysregulation. The spectrum of clinical features in patients with *PIK3CD* GOF mutations includes recurrent respiratory tract infections, lymphadenopathy, autoimmunity, EBV viremia, and B-cell lymphoma, many of which are EBV^+.[20, 21] Although the role and requirements of PI3K signaling in the setting of lymphocyte development, tolerance, and immunity have been established from studies of genetically modified mice, the mechanisms contributing to disease in patients with *PIK3CD* GOF mutations remain incompletely defined. Here we have focused on the development and effector function of $CD8^+$ T and NK cellswith a view of understanding aspects of immune dysregulation and susceptibility to EBV-induced disease.

The immunologic phenotype of patients with *PIK3CD* GOF mutations includes an expansion of $CD8^+$ T cells skewed toward a T_{EM} phenotype and a concomitantly reduced CD4/CD8 ratio.[17, 18, 19, 20, 21, 22] We have now substantially confirmed and extended these findings in a very large cohort of patients (n = 39) by discovering that surface receptors, including CD57, 2B4, CD160, PD-1, KLRG1, and HLA class I, are upregulated on $CD8^+$ T-cell subsetsfrom patients with *PIK3CD* GOF mutations. Furthermore, $CD8^+$ T cells from patients with *PIK3CD* GOF mutations exhibited increased expression of granzyme B and perforin, reduced expression of IL-2, increased apoptosis, and impaired cytotoxicity. The phenotype of $CD8^+$ T cells in patients with *PIK3CD*GOF mutations is reminiscent of exhausted or senescent-type $CD8^+$ T cells observed after chronic or persistent viral infection in mice[56] and human subjects,[38, 41, 42, 43, 44, 45, 48, 51, 57] or in patients with other monogenic immune dysregulatory conditions, including dedicator of cytokinesis 8 *(DOCK8)*deficiency[58] and Evan syndrome caused by mutations in tripeptidyl peptidase 2 *(TPP2)*.[40] Mouse models of persistent lymphocytic choriomeningitis virusinfection have demonstrated that $CD8^+$ T-cell function is compromised by ongoing viral stimulation, such that upregulation of inhibitory receptors and altered expression of effector cytokines underpins defective behavior of these cells.[37] Thus acquisition of an exhausted- or senescent-type phenotype by $CD8^+$T cells from patients with *PIK3CD* GOF mutations likely explains their impaired cytotoxicity, potentially resulting in reduced immunosurveillance of EBV-infected B cells and increased incidence of EBV-associated disease.[21] The exhausted or senescent phenotype and function of $CD8^+$ T cells in

patients with chronic infections, such as HIV, CMV, or hepatitis B or C virus, have been proposed to result from constant activation by persistent viral antigen.[37, 38, 57] It is likely that these parallel features of exhausted- or senescent-type $CD8^+$ T cells in patients with *PIK3CD* GOF mutations results from constitutive PI3K activation in these cells, essentially mimicking ongoing signaling through the TCR and costimulatory receptors rather than being secondary to recurrent or chronic pathogen infections. This is supported by the consistent exhausted- or senescent-type phenotype of $CD8^+$ T cells in EBV-naive subjects, as well as patients with mild and chronic EBV viremia, coupled with the finding of a similar $CD8^+$ T-cell phenotype in unimmunized/uninfected *Pik3cd*^{E1020K} mutant mice.

PIK3CD GOF mutations result in constitutive hyperactivation of the PI3K-AKT-mTOR pathway, thereby promoting aerobic glycolysis.[19] Previous studies demonstrated a link between aerobic glycolysis and susceptibility to RICD.[28] We also found increased susceptibility of $CD8^+$ T cells from patients with *PIK3CD*GOF mutations to RICD. Thus this altered metabolic state might partially cause accelerated T-cell effector generation, limited effector function, and increased sensitivity to RICD, culminating in the phenotype of $CD8^+$ T-cell dysfunction. Interestingly, susceptibility to RICD was observed for *PIK3CD* GOF T_{EM}, but not T_{EMRA}, $CD8^+$ T cells. This correlated with selectively increased expression of *FASLG* by *PIK3CD* GOF T_{EM} cells. Interestingly, HIV-specific T_{EM} cells preferentially undergo greater spontaneous and CD95-mediated apoptosis than other $CD8^+$ T-cell subsets; this was associated with increased expression of PD-1, CD95, and CD57. [43, 44] Remarkably, T_{EM} cells from patients with *PIK3CD*GOF mutations expressed the highest levels of PD-1, CD95, and CD57 of all $CD8^+$ T-cell subsets examined. This phenotype of *PIK3CD* GOF T_{EM} cells, coupled with preferential induction of high levels of *FASLG* in *PIK3CD* GOF T_{EM}cells and the requirement for Fas/Fas ligand interactions to regulate RICD,[29] likely explains increased RICD in these, but not *PIK3CD* GOF T_{EMRA}, cells. These findings also highlight that analysis of immune dysregulatory conditions caused by monogenic mutations can greatly inform our knowledge of similar immunopathologies occurring in the general population induced by extrinsic factors, such as infectious agents. This further underscores the utility of studying patients with *PIK3CD* GOF mutations as a valuable means of dissecting pathways and mechanisms regulating immunosenescence.[21] Our findings, combined with those associating aerobic glycolysis with RICD,[28] strongly support the utility of inhibitors of the PI3K pathway as therapeutic modalities for treating patients with *PIK3CD* GOF mutations. Indeed, treatment with the mTOR inhibitor rapamycin or the recently developed PI3K p110δ inhibitor leniolisib reduced the proportions of circulating $CD57^+$ T cells in a short-term trial of patients with *PIK3CD* GOF mutations (Edwards, Tangye, and Uzel).[19, 22]

Upregulation of molecules, including CD57, KLRG1, CD16, and killer cell immunoglobulin-like receptors (eg, CD158a/g/h), as well as the effector molecules granzyme B and perforin, is consistent with maturation of NK cells from a $CD56^{bright}$ to a $CD56^{dim}$ phenotype.[59] Stepwise reductions in NKG2A and increases in killer cell immunoglobulin-like receptor expression have been shown to correlate with NK cell terminal differentiation and IFN-γ production.[60]NK cells were present in normal proportions in patients with *PIK3CD* GOF mutations, with no effect on the distribution of cells between the $CD56^{bright}$ and $CD56^{dim}$ compartments. However, the activation status of the NK cells was aberrant, as indicated by increased expression of CD57, CD16, NKG2A, and CD158a/g/h and reduced cytotoxicity toward EBV-infected B cells. This dysregulated pattern of receptor expression might have an adverse effect on NK cell function in these patients, such as the observed reductions in cytotoxicity against EBV-LCLs. Our findings are largely consistent with very recently published findings that also reported normal or near-normal proportions of total NK cells, normal proportions of $CD56^{hi}$ and $CD56^{dim}$ subsets of NK cells, increased expression of NKG2A on $CD56^{dim}$ NK cells, and impaired cytotoxicity of NK cells from patients with *PIK3CD* GOF mutations.[61] Interestingly, we observed increased expression of granzymes and perforin by *PIK3CD* GOF $CD8^+$ T cells and NK cells but impaired cytotoxicity. These paradoxical findings can be explained by the recent discovery that NK cells from patients with *PIK3CD* GOF mutations exhibit poor polarization of the lytic machinery to the microtubule organizing center, a requisite step for cytotoxic function.[61] Thus our phenotypic and functional data suggest that *PIK3CD* GOF mutations compromise the mobilization and polarization of the lytic machinery in cytotoxic lymphocytes, impairing their cytotoxic effector function, despite increased expression of cytotoxic mediators.

The significance of an altered phenotype of $CD8^+$ T cells, NK cells, and B cells in patients with *PIK3CD* GOF mutations is highlighted by the known functions of several of these receptor/ligand pairs in host defense against EBV. 2B4 can act as an inhibitory or activating receptor,[46, 47] the outcome of which depends on its level of expression and engagement by CD48, as well as signaling through SAP.[62] Thus, on one hand, impaired signaling through 2B4 caused by SAP deficiency underlies defective cytolytic responses of $CD8^+$ T and NK cells to EBV in X-linked lymphoproliferative syndrome,46, 47 whereas on the other hand, overexpression or extensive cross-linking of 2B4 on cytotoxic cells results in inhibitory signaling.[62] Thus a fine balance between inputs through 2B4 needs to be achieved for 2B4 to function as an activating or inhibitory receptor, particularly with regard to fine-tuning of the $CD8^+$ T-cell response to antigen. In patients with *PIK3CD* GOF mutations, 2B4 expression was increased on $CD8^+$ T cells, yet SAP expression was normal. Heightened expression of CD48 on primary B cells and LCLs from patients with *PIK3CD* GOF mutations invokes a scenario in which increased cross-linking of 2B4 on $CD8^+$ T and NK cells would result in inhibitory signaling through this receptor. Modulation of this axis might prove useful in conditions in which 2B4 or CD48 expression is increased. Indeed, blockade of 2B4/CD48 interactions improved the *in vitro*effector function of exhausted-type hepatitis B virus-specific $CD8^+$ T cells.[51] Upregulation of PD-1 on $CD8^+$ T cells and PD-1 ligands on B cells in patients with *PIK3CD* GOF mutations revealed additional mechanisms of impaired cytolytic function in patients with *PIK3CD* GOF mutations, with engagement of PD-1 restraining the function of $CD8^+$ T cells.[37, 38] This also raises the possibility that PD-1 blockade, which improves or restores $CD8^+$ T-cell function in mouse models of chronic viral infection,[56] might be a therapeutic option to treat EBV viremia in patients with this disease. Such a proposition is supported by previous data from studies of HIV infection, in which $CD8^+$ T cells acquire an exhausted phenotype similar to that observed for patients with *PIK3CD* GOF mutations.[42, 43, 44, 45, 48] *In vitro* blockade of PD-1/PD-L1 interactions with specific mAbs restored proliferation and effector function of $CD8^+$ T cells in HIV^+subjects.[42, 44, 45, 48] Remarkably, effector function of these cells was further improved by combined blockade of PD-1 and 2B4.[48] Thus it is plausible that checkpoint inhibitors, which have found such great success in cancer immunotherapy, could have application in treating *PIK3CD* GOF. However, although checkpoint inhibitor–type therapies for treating patients with *PIK3CD*GOF mutations can revert the phenotype and function of exhausted/ senescent $CD8^+$ T cells in these subjects, their effects on the proinflammatory functions of immune cells would have to be closely monitored.

Overall, $CD8^+$ T cells in patients with *PIK3CD* GOF mutations, as well as a mouse model of this condition, present with features of accelerated differentiation, premature exhaustion, and/or immunosenescence with evidence of increased apoptosis and cytotoxic dysfunction accompanied by altered NK cell phenotype and defective cytotoxicity toward EBV-infected B cells. These observations parallel the aberrant expression of ligands for key regulatory molecules on B cells, highlighting the amenability of the CD48-2B4 and PD-1–PD-L1/2[42,45,48,51] axes to immunotherapeutic intervention as an alternative or complement to current therapies, such as rapamycin [19, 20] or leniolisib.[22] We are now also well placed to use our mouse model as a preclinical screen to test the efficacy of such putative therapeutics in restoring defects in $CD8^+$ T-cell development and differentiation caused by hyperactive PI3K signaling.

References

1 E.H. Kim, M. Suresh **Role of PI3K/Akt signaling in memory CD8 T cell differentiation** Front Immunol, 4 (2013), p. 20

2 D. Chantry, A. Vojtek, A. Kashishian, D.A. Holtzman, C. Wood, P.W. Gray, *et al.* **p110delta, a novel phosphatidylinositol 3-kinase catalytic subunit that associates with p85 and is expressed predominantly in leukocytes** J Biol Chem, 272 (1997), pp. 19236-19241

3 B. Vanhaesebroeck, M.J. Welham, K. Kotani, R. Stein, P.H. Warne, M.J. Zvelebil, *et al.* **P110delta, a novel phosphoinositide 3-kinase in leukocytes** Proc Natl Acad Sci U S A, 94 (1997), pp. 4330-4335

4 L.M. Sly, M.J. Rauh, J. Kalesnikoff, T. Buchse, G.S.H.I.P. Krystal **SHIP2, and PTEN activities are regulated in vivo by modulation of their protein levels: SHIP is up-regulated in macrophages and mast cells by lipopolysaccharide** Exp Hematol, 31 (2003), pp. 1170-1181

5 Y. Choi, J. Zhang, C. Murga, H. Yu, E. Koller, B.P. Monia, *et al.* **PTEN, but not SHIP and SHIP2, suppresses the PI3K/Akt pathway and induces growth inhibition and apoptosis of myeloma cells** Oncogene, 21 (2002), pp. 5289-5300

6 P.M. Gubser, G.R. Bantug, L. Razik, M. Fischer, S. Dimeloe, G. Hoenger, *et al.* **Rapid effector function of memory CD8+ T cells requires an immediate-early glycolytic switch** Nat Immunol, 14 (2013), pp. 1064-1072

7 D.K. Finlay **Regulation of glucose metabolism in T cells: new insight into the role of phosphoinositide 3-kinases** Front Immunol, 3 (2012), p. 247

8 X. Xu, L. Ye, K. Araki, R. Ahmed **mTOR, linking metabolism and immunity** Semin Immunol, 24 (2012), pp. 429-435

9 K. Yang, H. Chi**mTOR and metabolic pathways in T cell quiescence and functional activation** Semin Immunol, 24 (2012), pp. 421-428

10 K. Okkenhaug, A. Bilancio, G. Farjot, H. Priddle, S. Sancho, E. Peskett, *et al.* **Impaired B and T cell antigen receptor signaling in p110delta PI 3-kinase mutant mice** Science, 297 (2002), pp. 1031-1034

11 V.Q. Pearce, H. Bouabe, A.R. MacQueen, V. Carbonaro, K. Okkenhaug **PI3Kdelta regulates the magnitude of CD8+ T cell responses after challenge with *Listeria monocytogenes*** J Immunol, 195 (2015), pp. 3206-3217

12 A.L. Martin, M.D. Schwartz, S.C. Jameson, Y. Shimizu **Selective regulation of CD8 effector T cell migration by the p110 gamma isoform of phosphatidylinositol 3-kinase** J Immunol, 180 (2008), pp. 2081-2088

13 N. Kim, A. Saudemont, L. Webb, M. Camps, T. Ruckle, E. Hirsch, *et al.* **The p110delta catalytic isoform of PI3K is a key player in NK-cell development and cytokine secretion** Blood, 110 (2007), pp. 3202-3208

14 H. Guo, A. Samarakoon, B. Vanhaesebroeck, S. Malarkannan **The p110 delta of PI3K plays a critical role in NK cell terminal maturation and cytokine/chemokine generation** J Exp Med, 205 (2008), pp. 2419-2435

15 K. Jiang, B. Zhong, D.L. Gilvary, B.C. Corliss, E. Hong-Geller, S. Wei, *et al.* **Pivotal role of phosphoinositide-3 kinase in regulation of cytotoxicity in natural killer cells** Nat Immunol, 1 (2000), pp. 419-425

16 J.S. Oak, D.A. Fruman **Role of phosphoinositide 3-kinase signaling in autoimmunity** Autoimmunity, 40 (2007), pp. 433-441

17 C.L. Lucas, A. Chandra, S. Nejentsev, A.M. Condliffe, K. Okkenhaug **PI3Kdelta and primary immunodeficiencies** Nat Rev Immunol, 16 (2016), pp. 702-714

18 I. Angulo, O. Vadas, F. Garcon, E. Banham-Hall, V. Plagnol, T.R. Leahy, *et al.* **Phosphoinositide 3-kinase delta gene mutation predisposes to respiratory infection and airway damage** Science, 342 (2013), pp. 866-871

19 C.L. Lucas, H.S. Kuehn, F. Zhao, J.E. Niemela, E.K. Deenick, U. Palendira, *et al.* **Dominant-activating germline mutations in the gene encoding the PI(3)K catalytic subunit p110delta result in T cell senescence and human immunodeficiency** Nat Immunol, 15 (2014), pp. 88-97

20 T.I. Coulter, A. Chandra, C.M. Bacon, J. Babar, J. Curtis, N. Screaton, *et al.* **Clinical spectrum and features of activated phosphoinositide 3-kinase delta syndrome: a large patient cohort study** J Allergy Clin Immunol, 139 (2017), pp. 597-606.e4

21 J.M. Carpier, C.L. Lucas **Epstein-Barr Virus susceptibility in activated PI3Kdelta syndrome (APDS) immunodeficiency** Front Immunol, 8 (2018), p. 2005

22 V.K. Rao, S. Webster, V. Dalm, A. Sediva, P.M. van Hagen, S. Holland, *et al.* **Effective "activated PI3Kdelta syndrome"-targeted therapy with the PI3Kdelta inhibitor leniolisib** Blood, 130 (2017), pp. 2307-2316

23 A.J. Takeda, Y. Zhang, G.L. Dornan, B.D. Siempelkamp, M.L. Jenkins, H.F. Matthews, *et al.* **Novel PIK3CD mutations affecting N-terminal residues of p110delta cause activated PI3Kdelta syndrome (APDS) in humans** J Allergy Clin Immunol, 140 (2017), pp. 1152-1156.e10

24 A.E. Dulau Florea, R.C. Braylan, K.T. Schafernak, K.W. Williams, J. Daub, R.K. Goyal, *et al.* **Abnormal B-cell maturation in the bone marrow of patients with germline mutations in PIK3CD** J Allergy Clin Immunol, 139 (2017), pp. 1032-1035.e6

25 D.A. Price, J.M. Brenchley, L.E. Ruff, M.R. Betts, B.J. Hill, M. Roederer, *et al.* **Avidity for antigen shapes clonal dominance in CD8+ T cell populations specific for persistent DNA viruses** J Exp Med, 202 (2005), pp. 1349-1361

26 B. Chaigne-Delalande, F.Y. Li, G.M. O'Connor, M.J. Lukacs, P. Jiang, L. Zheng, *et al.* **Mg2+ regulates cytotoxic functions of NK and CD8 T cells in chronic EBV infection through NKG2D** Science, 341 (2013), pp. 186-191

27 H. Abolhassani, E.S. Edwards, A. Ikinciogullari, H. Jing, S. Borte, M. Buggert, *et al.* **Combined immunodeficiency and Epstein-Barr virus-induced B cell malignancy in humans with inherited CD70 deficiency** J Exp Med, 214 (2017), pp. 91-106

28 S.E. Larsen, A. Bilenkin, T.N. Tarasenko, S. Arjunaraja, J.R. Stinson, P.J. McGuire, *et al.* **Sensitivity to restimulation-induced cell death is linked to glycolytic metabolism in human T cells** J Immunol, 198 (2017), pp. 147-155

29 A.L. Snow, R.A. Marsh, S.M. Krummey, P. Roehrs, L.R. Young, K. Zhang, *et al.* **Restimulation-induced apoptosis of T cells is impaired in patients with X-linked lymphoproliferative disease caused by SAP deficiency** J Clin Invest, 119 (2009), pp. 2976-2989

30 T.D. Chan, D. Gatto, K. Wood, T. Camidge, A. Basten, R. Brink **Antigen affinity controls rapid T-dependent antibody production by driving the expansion rather than the differentiation or extrafollicular migration of early plasmablasts** J Immunol, 183 (2009), pp. 3139-3149

31 G. Bucciol, L. Willems, E. Hauben, A. Uyttebroeck, M. Proesmans, I. Meyts **Thyroid carcinoma in a child with activated phosphoinositide 3-kinase delta syndrome: somatic effect of a germline mutation** J Clin Immunol, 37 (2017), pp. 422-426

32 K. Jentsch-Ullrich, M. Koenigsmann, M. Mohren, A. Franke **Lymphocyte subsets' reference ranges in an age- and gender-balanced population of 100 healthy adults—a monocentric German study** Clin Immunol, 116 (2005), pp. 192-197

33 F. Sallusto, D. Lenig, R. Forster, M. Lipp, A. Lanzavecchia **Two subsets of memory T lymphocytes with distinct homing potentials and effector functions** Nature, 401 (1999), pp. 708-712

34 L. Gattinoni, E. Lugli, Y. Ji, Z. Pos, C.M. Paulos, M.F. Quigley, *et al.* **A human memory T cell subset with stem cell-like properties** Nat Med, 17 (2011), pp. 1290-1297

35 J.M. Brenchley, N.J. Karandikar, M.R. Betts, D.R. Ambrozak, B.J. Hill, L.E. Crotty, *et al.* **Expression of CD57 defines replicative senescence and antigen-induced apoptotic death of CD8+ T cells** Blood, 101 (2003), pp. 2711-2720

36 L. Papagno, C.A. Spina, A. Marchant, M. Salio, N. Rufer, S. Little, *et al.* **Immune activation and CD8+ T-cell differentiation towards senescence in HIV-1 infection** PLoS Biol, 2 (2004), p. E20

37 E.J. Wherry, M. Kurachi **Molecular and cellular insights into T cell exhaustion** Nat Rev Immunol, 15 (2015), pp. 486-499

38 I.S. Okoye, M. Houghton, L. Tyrrell, K. Barakat, S. Elahi **Coinhibitory receptor expression and immune checkpoint blockade: maintaining a balance in CD8(+) T cell responses to chronic viral infections and cancer** Front Immunol, 8 (2017), p. 1215

39 L. Kestens, G. Vanham, P. Gigase, G. Young, I. Hannet, F. Vanlangendonck, *et al.* **E xpression of activation antigens, HLA-DR and CD38, on CD8 lymphocytes during HIV-1 infection** AIDS, 6 (1992), pp. 793-797

40 P. Stepensky, A. Rensing-Ehl, R. Gather, S. Revel-Vilk, U. Fischer, S. Nabhani, *et al.* **Early-onset Evans syndrome, immunodeficiency, and premature immunosenescence associated with tripeptidyl-peptidase II deficiency** Blood, 125 (2015), pp. 753-761

41 B. Bengsch, B. Seigel, M. Ruhl, J. Timm, M. Kuntz, H.E. Blum, *et al.* **Coexpression of PD-1, 2B4, CD160 and KLRG1 on exhausted HCV-specific CD8+ T cells is linked to antigen recognition and T cell differentiation** PLoS Pathog, 6 (2010), p. e1000947

42 C.L. Day, D.E. Kaufmann, P. Kiepiela, J.A. Brown, E.S. Moodley, S. Reddy, *et al.* **PD-1 expression on HIV-specific T cells is associated with T-cell exhaustion and disease progression** Nature, 443 (2006), pp. 350-354

43 C. Petrovas, J.P. Casazza, J.M. Brenchley, D.A. Price, E. Gostick, W.C. Adams, *et al.* **PD-1 is a regulator of virus-specific CD8+ T cell survival in HIV infection** J Exp Med, 203 (2006), pp. 2281-2292

44 C. Petrovas, B. Chaon, D.R. Ambrozak, D.A. Price, J.J. Melenhorst, B.J. Hill, *et al.* **Differential association of programmed death-1 and CD57 with ex vivo survival of CD8+ T cells in HIV infection** J Immunol, 183 (2009), pp. 1120-1132

45 L. Trautmann, L. Janbazian, N. Chomont, E.A. Said, S. Gimmig, B. Bessette, *et al.* **Upregulation of PD-1 expression on HIV-specific CD8+ T cells leads to reversible immune dysfunction** Nat Med, 12 (2006), pp. 1198-1202

46 A.D. Hislop, U. Palendira, A.M. Leese, P.D. Arkwright, P.S. Rohrlich, S.G. Tangye, *et al.* **I mpaired Epstein-Barr virus-specific CD8+ T-cell function in X-linked lymphoproliferative disease is restricted to SLAM family-positive B-cell targets** Blood, 116 (2010), pp. 3249-3257

47 U. Palendira, C. Low, A. Chan, A.D. Hislop, E. Ho, T.G. Phan, *et al.* **Molecular pathogenesis of EBV susceptibility in XLP as revealed by analysis of female carriers with heterozygous expression of SAP** PLoS Biol, 9 (2011), p. e1001187

48 T. Yamamoto, D.A. Price, J.P. Casazza, G. Ferrari, M. Nason, P.K. Chattopadhyay, *et al.* **Surface expression patterns of negative regulatory molecules identify determinants of virus-specific CD8+ T-cell exhaustion in HIV infection** Blood, 117 (2011), pp. 4805-4815

49 M.F. Callan, L. Tan, N. Annels, G.S. Ogg, J.D. Wilson, C.A. O'Callaghan, *et al.* **Direct visualization of antigen-specific CD8+ T cells during the primary immune response to Epstein-Barr virus In vivo** J Exp Med, 187 (1998), pp. 1395-1402

50 A.D. Hislop, N.E. Annels, N.H. Gudgeon, A.M. Leese, A.B. Rickinson **Epitope-specific evolution of human CD8(+) T cell responses from primary to persistent phases of Epstein-Barr virus infection** J Exp Med, 195 (2002), pp. 893-905

51 B. Raziorrouh, W. Schraut, T. Gerlach, D. Nowack, N.H. Gruner, A. Ulsenheimer, *et al.* **The immunoregulatory role of CD244 in chronic hepatitis B infection and its inhibitory potential on virus-specific CD8+ T-cell function** Hepatology, 52 (2010), pp. 1934-1947

52 O. Chijioke, A. Muller, R. Feederle, M.H. Barros, C. Krieg, V. Emmel, *et al.* **Human natural killer cells prevent infectious mononucleosis features by targeting lytic Epstein-Barr virus infection** Cell Rep, 5 (2013), pp. 1489-1498

53 T. Azzi, A. Lunemann, A. Murer, S. Ueda, V. Beziat, K.J. Malmberg, *et al.* **Role for early-differentiated natural killer cells in infectious mononucleosis** Blood, 124 (2014), pp. 2533-2543

54 S.M. Lens, P. Drillenburg, B.F. den Drijver, G. van Schijndel, S.T. Pals, R.A. van Lier, *et al.* **Aberrant expression and reverse signalling of CD70 on malignant B cells** Br J Haematol, 106 (1999), pp. 491-503

55 D.J. Andorsky, R.E. Yamada, J. Said, G.S. Pinkus, D.J. Betting, J.M. Timmerman **Programmed death ligand 1 is expressed by non-hodgkin lymphomas and inhibits the activity of tumor-associated T cells** Clin Cancer Res, 17 (2011), pp. 4232-4244

56 E.J. Wherry, S.J. Ha, S.M. Kaech, W.N. Haining, S. Sarkar, V. Kalia, *et al.* **Molecular signature of CD8+ T cell exhaustion during chronic viral infection** Immunity, 27 (2007), pp. 670-684

57 W. Tu, S. Rao **Mechanisms underlying T cell immunosenescence: aging and cytomegalovirus infection** Front Microbiol, 7 (2016), p. 2111

58 K.L. Randall, S.S. Chan, C.S. Ma, I. Fung, Y. Mei, M. Yabas, *et al.* **DOCK8 deficiency impairs CD8 T cell survival and function in humans and mice** J Exp Med, 208 (2011), pp. 2305-2320

59 C.M. Nielsen, M.J. White, M.R. Goodier, E.M. Riley **Functional significance of CD57 expression on human NK Cells and relevance to disease** Front Immunol, 4 (2013), p. 422

60 V. Beziat, B. Descours, C. Parizot, P. Debre, V. Vieillard **NK cell terminal differentiation: correlated stepwise decrease of NKG2A and acquisition of KIRs** PLoS One, 5 (2010), p. e11966

61 R. Ruiz-Garcia, A. Vargas-Hernandez, I.K. Chinn, L.S. Angelo, T.N. Cao, Z. Coban-Akdemir, *et al.* **Mutations in PI3K110delta cause impaired natural killer cell function partially rescued by rapamycin treatment** J Allergy Clin Immunol (2018)

62 L.K. Chlewicki, C.A. Velikovsky, V. Balakrishnan, R.A. Mariuzza, V. Kumar **Molecular basis of the dual functions of 2B4 (CD244)** J Immunol, 180 (2008), pp. 8159-8167

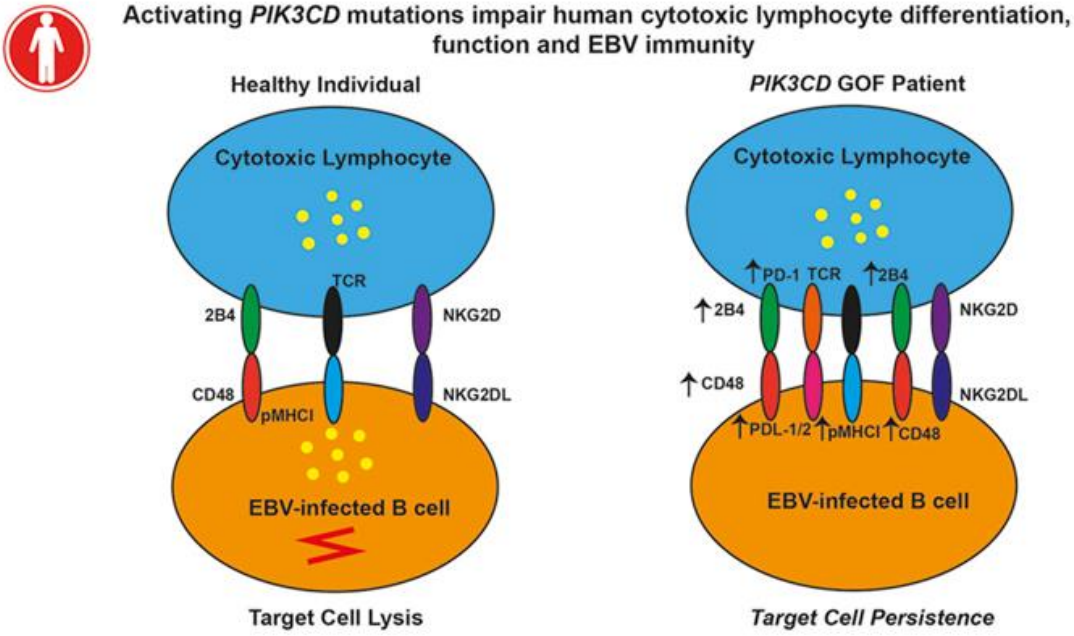

Abbreviations

EBV	Epstien-Barr Virus
GOF	Gain-of-Function
NKG2D	Natural-Killer Group 2, Member D
NKG2DL	NKG2D Ligand
2B4	Natural Killer Receptor 2B4
PD-1	Programmed Death Receptor-1
PDL1/2	Programmed Death Ligand 1/2
pMHCI	peptide Major Histocompatibility Complex I
TCR	T-cell Receptor

Figure 1

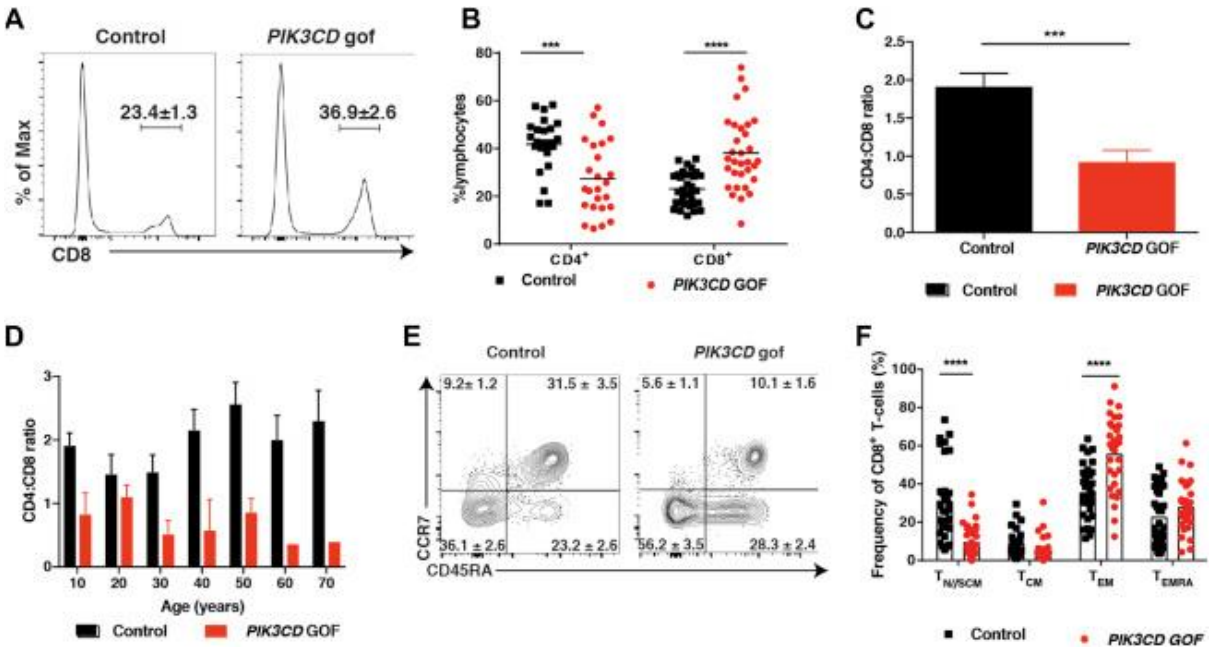

T_{EM} cell skewing of $CD8^+$ T lymphocytes in patients with *PIK3CD* GOF mutations. PBMCs from healthy control subjects (n = 33) and patients with *PIK3CD* GOF mutations (n = 33) were labeled with mAbs against CD4, CD8, CCR7, and CD45RA. **A,** Representative histogram plots showing CD8 expression by lymphocytes from control subjects and patients with *PIK3CD* GOF mutations. **B,** Frequency of $CD4^+$ or $CD8^+$ T cells within the lymphocyte gate in control subjects and patients with *PIK3CD* GOF mutations. Each *symbol* corresponds to an individual donor or patient; the *horizontal bar*represents the mean. **C** and **D,** Ratio of $CD4^+$ to $CD8^+$ T cells in all control subjects and patients with *PIK3CD* GOF mutations (Fig 1, *C*) or control subjects and patients with *PIK3CD* GOF mutations according to age (Fig 1, *D*). **E** and **F,** T_N/T_{SCM} ($CCR7^+CD45RA^+$), T_{CM} ($CCR7^+CD45RA^-$), T_{EM} ($CCR7^-CD45RA^-$), and T_{EMRA} ($CCR7^-CD45RA^+$) $CD8^+$ T cells were identified. Fig 1, *E*, Representative fluorescence-activated cell sorting plots of CD45RA- and CCR7-expressing populations in $CD8^+$ T cells from control subjects and patients with *PIK3CD* GOF mutations. Fig 1, *F*, Frequency of T_N/T_{SCM}, T_{CM}, T_{EM}, and T_{EMRA} $CD8^+$ T cells in control subjects and patients with *PIK3CD* GOF mutations. Statistics were performed by using the *t* test with the Mann-Whitney test (Fig 1, *B* and *C*) or 2-way ANOVA (Fig 1, *F*). ***$P < .01$ and ****$P < .0001$.

Figure 2

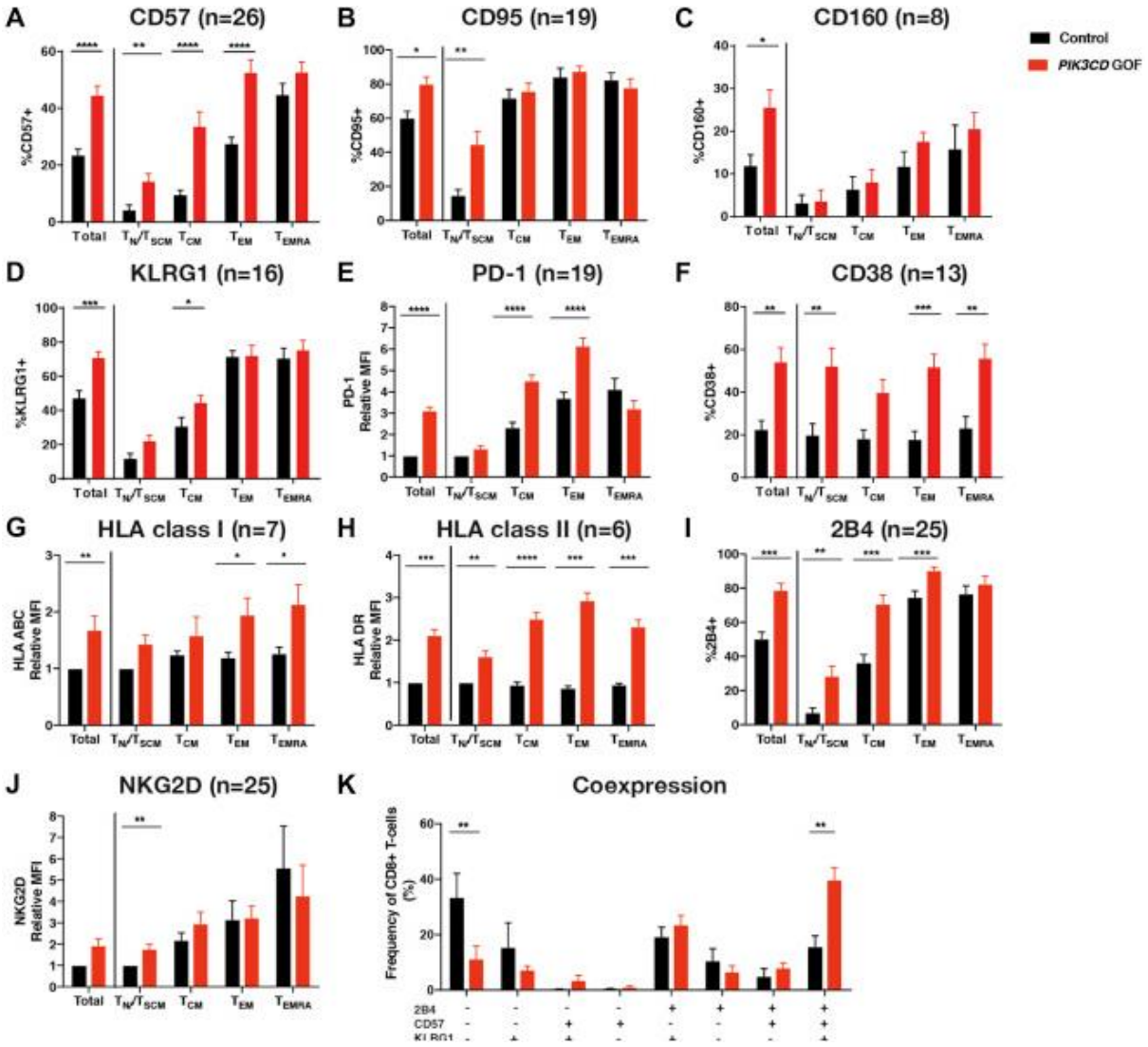

CD8⁺ T cells in patients with *PIK3CD* GOF mutations acquire an exhausted-type phenotype. PBMCs from healthy control subjects and patients with *PIK3CD* GOF mutations were labeled with mAbsagainst CD8, CD45RA, CCR7, CD57, 2B4, NKG2D, CD95, KLRG1, PD-1, CD38, HLA class I (HLA-ABC), and HLA class II (HLA-DR). **A-J,** Total CD8⁺ T cells, as well as T_N/T_{SCM} ($CCR7^+CD45RA^+$), T_{CM}($CCR7^+CD45RA^-$), T_{EM} ($CCR7^-CD45RA^-$), and T_{EMRA} ($CCR7^-CD45RA^+$) subsets, were delineated, and the frequency of each population expressing CD57 (Fig 2, *A*), CD95 (Fig 2, *B*), CD160 (Fig 2, *C*), or KLRG1 (Fig 2, *D*); relative expression of PD-1 (Fig 2, *E*); percentage of CD38⁺ cells (Fig 2, *F*); relative expression of HLA class I (Fig 2, *G*) and HLA class II (Fig 2, *H*); percentage of 2B4⁺ cells (Fig 2, *I*); and relative expression of NKG2D (Fig 2, *J*) were determined. Relative expression is depicted as the fold change in mean fluorescence intensity compared with either total or naive CD8⁺ T cells from healthy subjects. Values *(n)* in each panel represent numbers of healthy control subjects and patients with *PIK3CD* GOF mutations examined for each indicated surface marker. **K,** Coexpression of CD57, KLRG1, and 2B4 on CD8⁺ T cells. Statistics were performed by using 2-way ANOVA. **P* < .05, ***P* < .01, ****P* < .001, and *****P* < .0001.

Figure 3

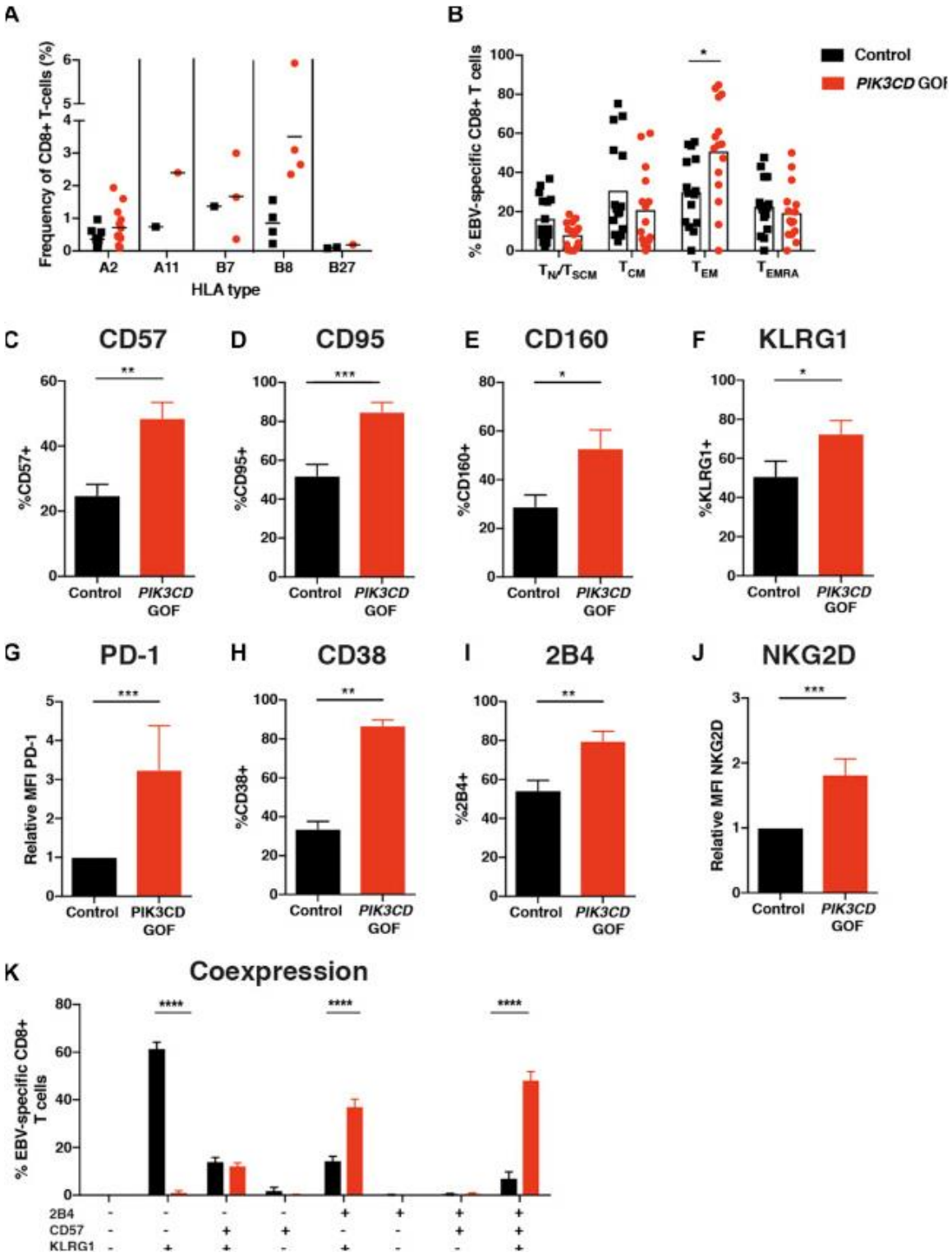

EBV-specific CD8⁺ T cells exhibit perturbed expression of regulatory molecules in patients with *PIK3CD* GOF mutations. **A** and **B,** PBMCs from patients with *PIK3CD* GOF mutations (n = 14) and HLA-matched control subjects (n = 14) were incubated with specific EBV–peptide–MHC class I tetramer complexes (Table E1) together with mAbs against CD8, CD45RA, CCR7, CD57, 2B4, CD160, NKG2D, CD95, KLRG1, PD-1, or CD38. Fig 3, *A*, Frequency of EBV-specific CD8⁺ T cells in healthy subjects and patients with *PIK3CD* GOF mutations. Fig 3, *B*, Distribution of EBV tetramer-positive CD8⁺ T cells in T_N/T_{SCM}, T_{CM}, T_{EM}, and T_{EMRA} CD8⁺ T-cell populations in healthy control subjects and patients with *PIK3CD* GOF mutations. Statistics were performed by using 2-way ANOVA. **C-J,** Frequency of EBV-specific CD8⁺ T cells expressing CD57 (Fig 3, *C*), CD95 (Fig 3, *D*), CD160 (Fig 3, *E*), and KLRG1 (Fig 3, *F*); relative expression of PD-1 (Fig 3, *G*); percentage expressing CD38 (Fig 3, *H*) and 2B4 (Fig 3, *I*); and relative expression of NKG2D (Fig 3, *J*) on EBV-specific CD8⁺ T cells from patients with *PIK3CD* GOF mutations and control subjects were determined. Relative expression is depicted as fold change compared with mean fluorescence intensity of EBV-specific CD8⁺ T cells from healthy donors. Statistics were performed by using *t* tests with Mann-Whitney tests. **K,** Coexpression of CD57, KLRG1, and 2B4 in EBV-specific CD8⁺ T cells. Statistics were performed by using 2-way ANOVA. **P* < .05, ***P* < .01, ****P* < .001, and *****P* < .0001.

Figure 4

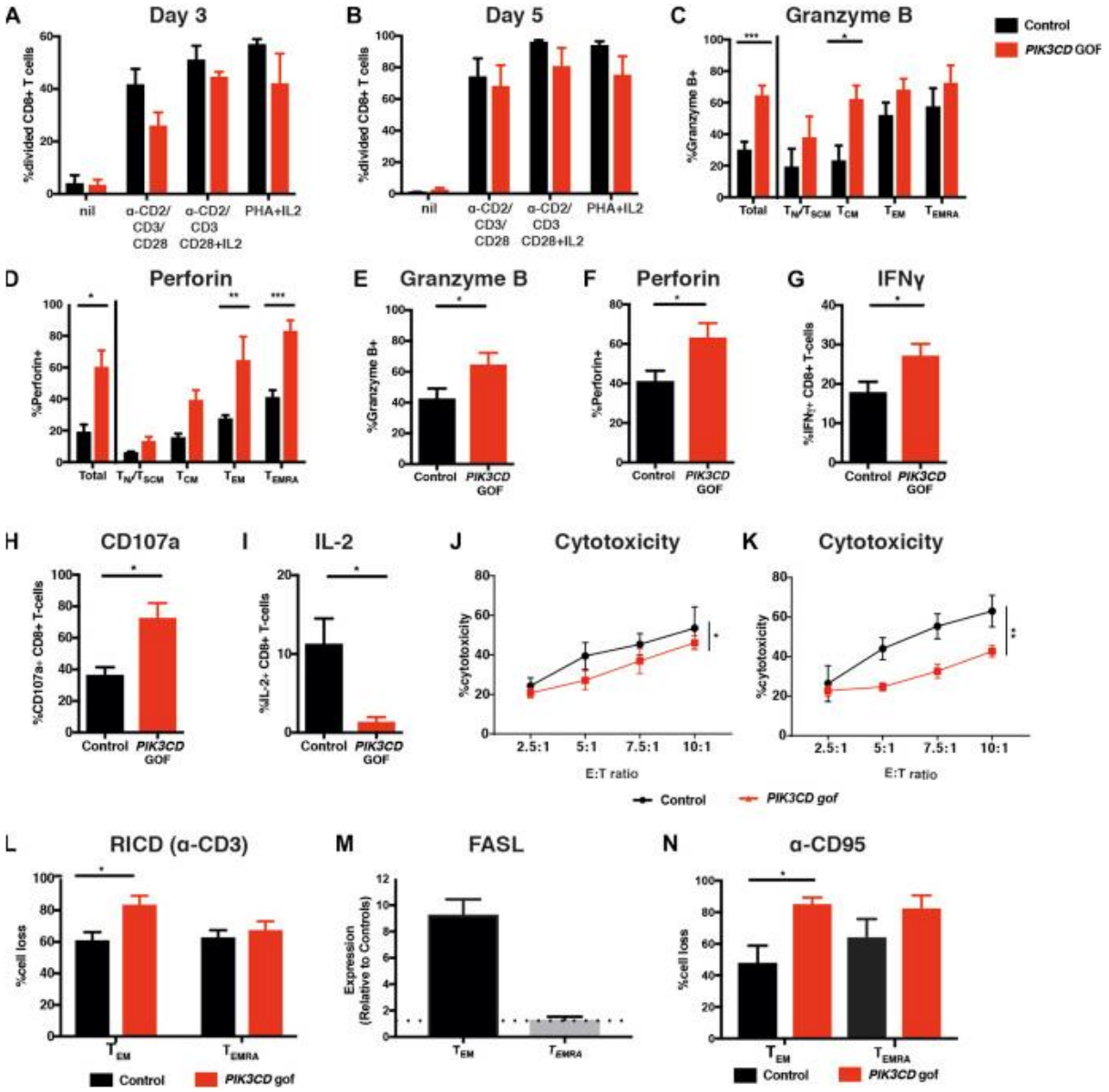

Altered functionality of CD8⁺ T cells and enhanced restimulation-induced cell death of T_{EM} CD8⁺ T cells from patients with *PIK3CD* GOF mutations. **A** and **B,** PBMCs from healthy donors (n = 3-5) or patients with *PIK3CD* GOF mutations (n = 3-6) were labeled with carboxyfluorescein succinimidyl esterand stimulated *in vitro* in the absence *(nil)* or presence of mAbs specific for CD2, CD3, and CD28 with or without IL-2 or PHA/IL-2. Proliferation was determined after 3 (Fig 4, *A*) or 5 (Fig 4, *B*) days by calculating the percentage of CD8⁺ T cells that have undergone 2 or more divisions. Values represent means ± SEMs. **C** and **D,** PBMCs from patients with *PIK3CD* GOF mutations (n = 5-8) and healthy control subjects (n = 5-8) were stained directly *ex vivo* with mAbs to CD8, CCR7, CD45RA, granzyme B, and perforin. Frequency of CD8⁺ T cells expressing granzyme B (Fig 4, *C*) or perforin (Fig 4, *D*). Statistics were performed by using 2-way ANOVA. **E** and **F,** Frequency of EBV tetramer-positive CD8⁺ T cells expressing granzyme B (Fig 4, *E*) or perforin (Fig 4, *F*; n = 5). **G-I,** PBMCs from healthy control subjects (n = 6) and patients with *PIK3CD* GOF mutations (n = 6) were stimulated for 14 hours in the absence or presence of PMA/ionomycin with Brefeldin A and monensin. Percentage cells expressing IFN-γ (Fig 4, *G*), CD107a (Fig 4, *H*), or IL-2 (Fig 4, *I*) were determined. Statistics were performed by using t tests with Mann-Whitney tests. **J** and **K,** Percentage lysis of autologous LCLs by EBV-specific CD8⁺ T cells from healthy control subjects and patients with *PIK3CD* GOF mutations. Each graph depicts data from experiments using cells from 2 different patients and control subject run in triplicates. Statistics were performed by using 2-way ANOVA. **P* < .05, ***P* < .01, and ****P* < .001. **L-N,** Sorted T_{EM} and T_{EMRA} cells from healthy donors and patients with *PIK3CD* GOF mutations (n = 3) were stimulated with anti-CD2/CD3/CD28 mAbs and IL-2 for 10 days. Cells were then restimulated with plate-bound α-CD3 mAb to induce RICD or α-CD95 mAb for 24 hours, and cell death was assessed by staining with Zombie dye. Fig 4, *L*, Percentage death of T_{EM} and T_{EMRA} cells stimulated with α-CD3. Fig 4, *M*, *FASLG* expression 4 hours after α-CD3 mAb stimulation of sorted and activated T_{EM} and T_{EMRA} cell populations from patients with *PIK3CD* GOF mutations. Values represent mean ± SEM mRNA levels of *PIK3CD* GOF $T_{EM}$and T_{EMRA} cell populations relative to that expressed by corresponding cells from healthy control subjects (normalized to 1, as indicated by *dotted line*). Fig 4, *N*, Percentage death of T_{EM} and T_{EMRA} cells in response to 20 ng/mL α-CD95 mAb. Statistics were performed by using 2-way ANOVA. **P* < .05.

Figure 5

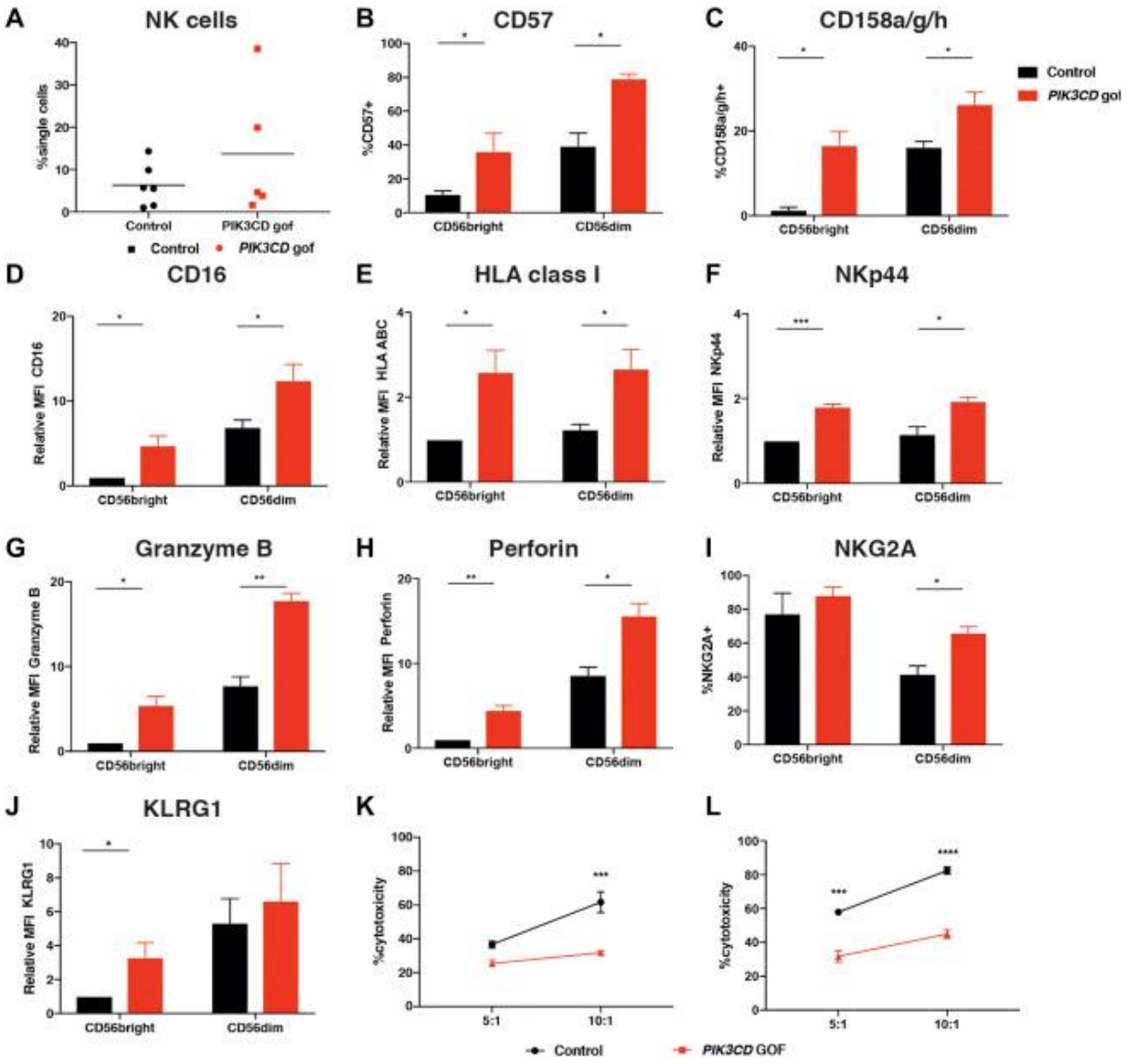

Impaired cytotoxicity of NK cells from patients with *PIK3CD* GOF mutations against EBV-B cell targets. **A-J,** PBMCs from healthy donors (n = 4-5) and patients with *PIK3CD* GOF mutations (n = 4-5) were labeled with mAbs against CD3, CD56, CD57, CD158a/g/h, CD16, HLA class I, NKp44, granzyme B, perforin, NKG2A (CD159a) and KLRG1. Fig 5, *A*, Frequency of NK cells ($CD3^{-}CD56^{+}$) in healthy control subjects and patients with *PIK3CD* GOF mutations. Frequency of $CD56^{bright}$ and $CD56^{dim}$ NK cells expressing CD57 (Fig 5, *B*) and CD158a/g/h (Fig 5, *C*) is shown. Relative expression of CD16 (Fig 5, *D*), HLA class I (HLA-ABC; Fig 5, *E*), NKp44 (Fig 5, *F*), granzyme B (Fig 5, *G*), perforin (Fig 5, *H*), frequency of NKG2A (CD159a; Fig 5, *I*); and relative expression of KLRG1 on $CD56^{bright}$ and $CD56^{dim}$ NK (Fig 5, *J*) cells from healthy control subjects and patients with *PIK3CD* GOF mutations are shown. Relative expression is presented as fold change over mean fluorescence intensity of $CD56^{bright}$ NK cells from healthy subjects. **K** and **L,** Percentage lysis of autologous LCLs by lymphokine-activated killer cells from patients with *PIK3CD* GOF mutations and healthy control subjects. Data are means ± SDs of experiments run in triplicates. Statistics were performed by using 2-way ANOVA. **P* < .05, ***P* < .01, ****P* < .001, and *****P* < .0001.

Figure 6

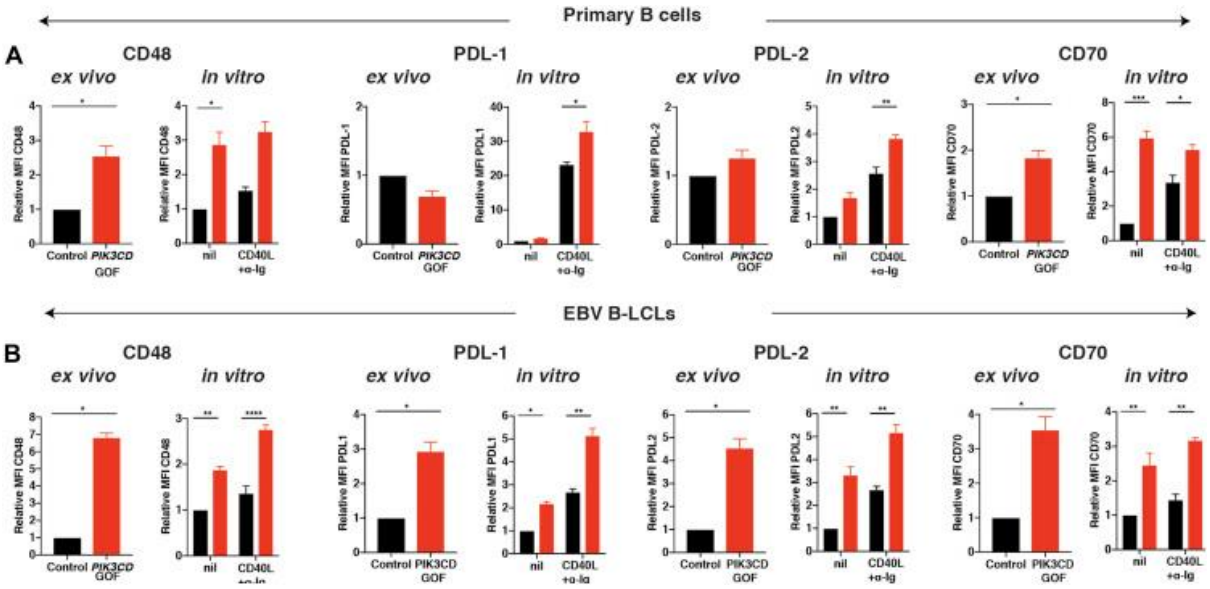

Modified ligand expression on B cells from patients with *PIK3CD* GOF mutations. **A** and **B,** Total peripheral blood B cells (Fig 6, *A*) or LCLs (Fig 6, *B*) from healthy subjects or patients with *PIK3CD* GOF mutations were either stained immediately *(left-hand plots)* or stimulated in the absence *(nil)* or presence of CD40 ligand *(CD40L)*/α-immunoglobulin *(right-hand plots)*; after 3 days, cells were stained with mAbsto CD48, PD-L1, PD-L2, or CD70. Graphs depict fold change of mean fluorescence intensity of the indicated molecules on primary B cells or LCLs from patients with *PIK3CD* GOF mutations relative to unstimulated B cells or LCLs from healthy control subjects. Statistics were performed by using 2-way ANOVA. **P* < .05, ***P* < .01, ****P* < .001, and *****P* < .0001.

Figure 7

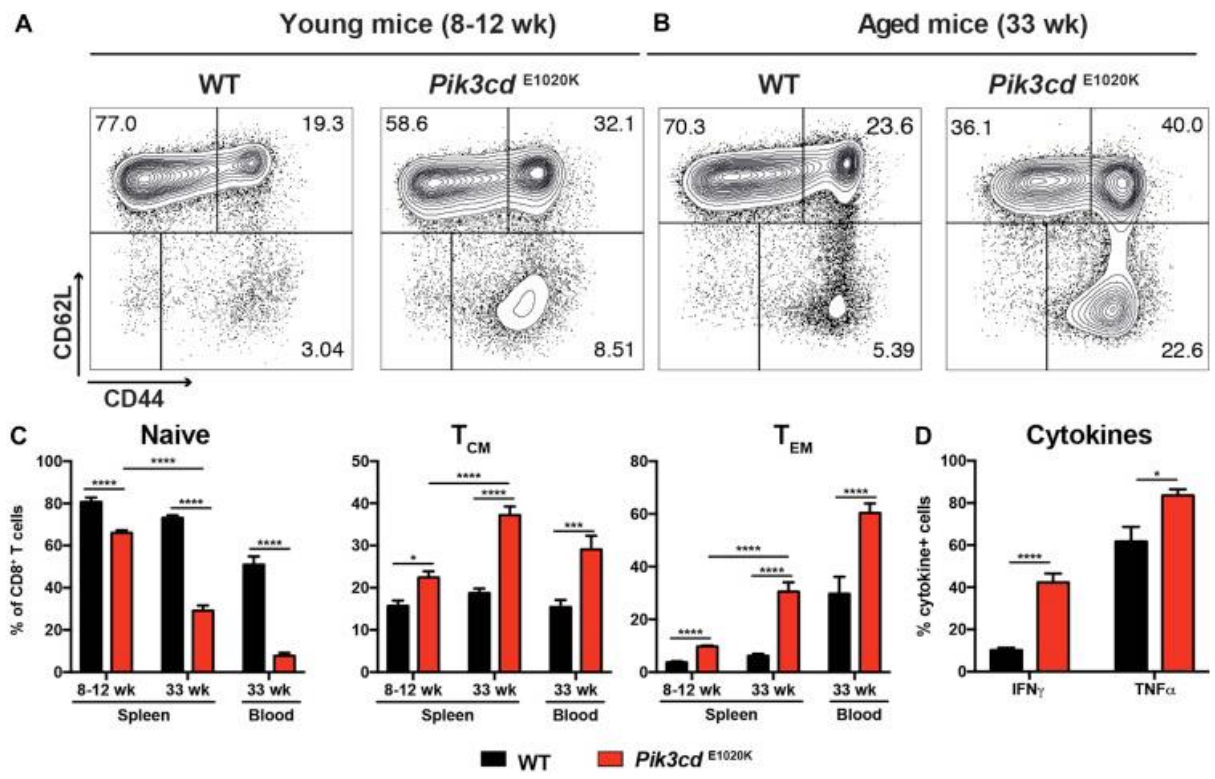

Pik3cd^{E1020K} mice exhibit phenotypic and functional defects in CD8$^+$ T cells independent of infection. **A-C,** Spleens or blood from wild-type *(WT)* and *Pik3cd*^{E1021K} mice at various ages were stained to identify different CD8$^+$ T-cell populations. Flow plots show representative staining of CD8$^+$ T cells from 8 to 12 weeks (WT, n = 10; *Pik3cd*,^{E1021K} n = 13; Fig 7, *A*) or 33-week-old mice (spleens, n = 11; blood, n = 6; Fig 7, *B*). Fig 7, *C*, Percentages of CD4$^+$ T cells with a T_N (CD44^{lo}CD62L^{hi}), T_{CM} (CD44^{hi}CD62L^{hi}), or T_{EM} (CD44^{hi}CD62L^{lo}) phenotype are shown in graphs (plots show means ± SEMs). **D,** Naive CD8$^+$ T cells were sorted from spleens of WT or *Pik3cd*^{E1021K} mice and cultured for 4 days with anti-CD3 and anti-CD28. Cells were then restimulated with PMA/ionomycin and IFN-γ and TNF-α production assessed (plots show means ± SEMs, n = 4-5). Significant differences were determined by using multiple *t* tests or 2-way ANOVA. **P* < .05, ****P* < .001, and *****P* < .0001.

Figure E1

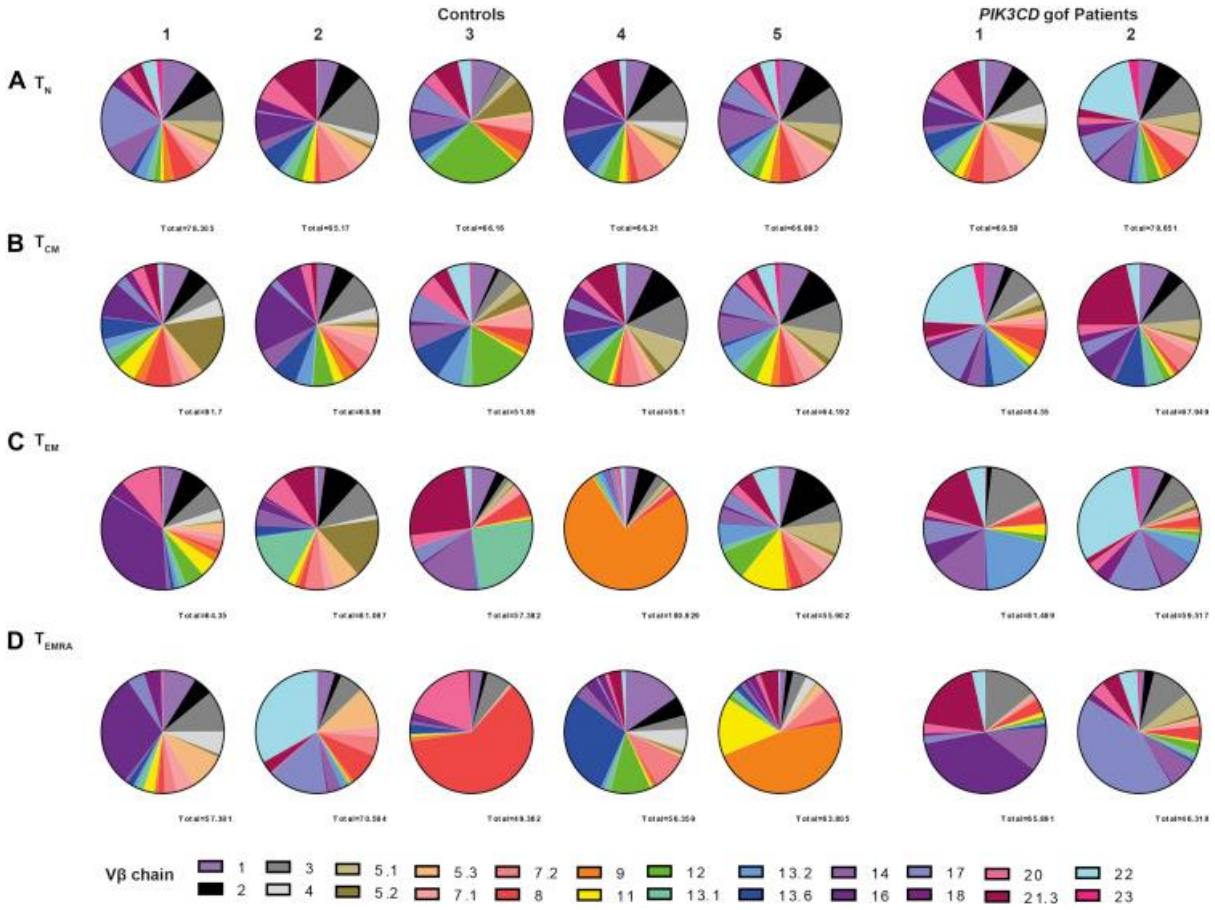

Vβ use of T-cell subsets from patients with *PIK3CD* GOF mutations. Samples from healthy donors (n = 5) and patients with *PIK3CD* GOF mutations (n = 2) were stained with Vβ mAbs in conjunction with mAbs to CD8, CD45RA, and CCR7 to determine the breadth of Vβ use by $CD8^+$ T-cell subsets in patients compared with control subjects: **A,** T_N ($CCR7^+CD45RA^+$); **B,** T_{CM} ($CCR7^+CD45RA^-$); **C,** T_{EM}($CCR7^-CD45RA^-$); and **D,** T_{EMRA} ($CCR7^-CD45RA^+$).

Figure E2

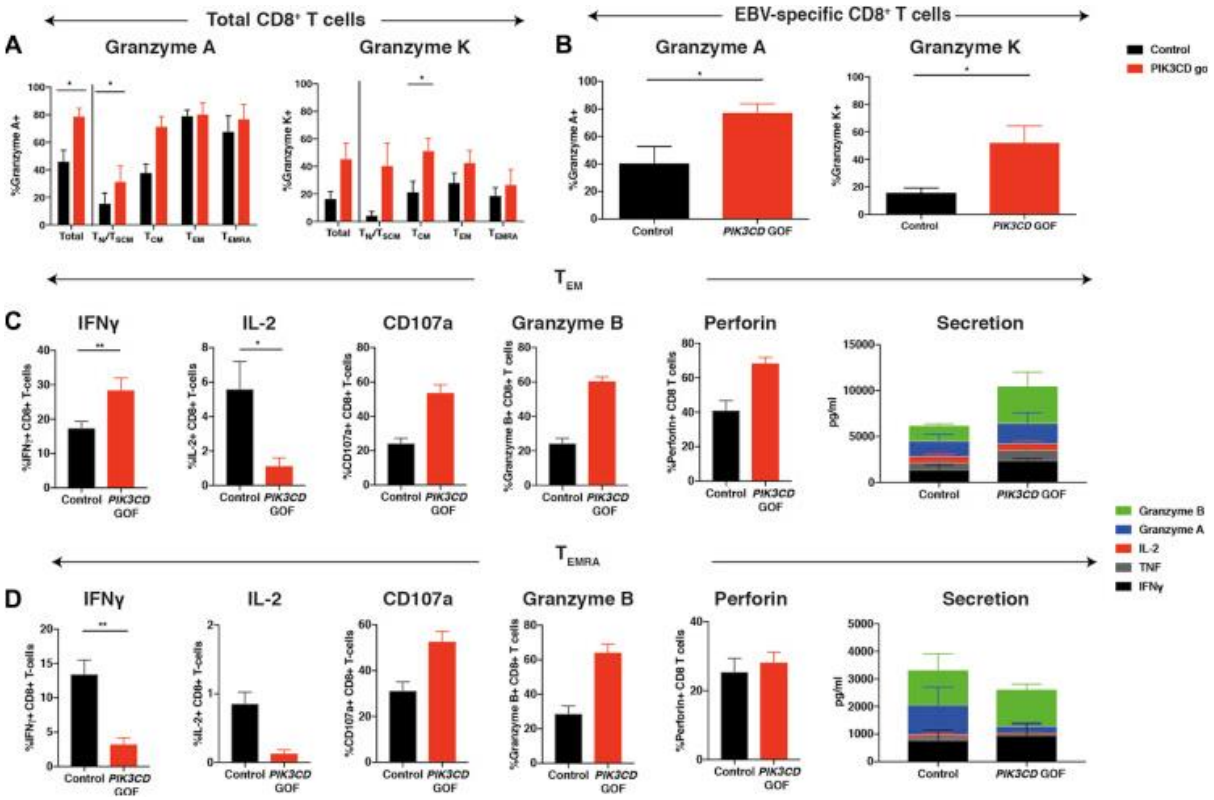

Altered cytokine production by T_{EM} and T_{EMRA} cells from patients with *PIK3CD* GOF mutations. **A**and **B,** Frequencies of total (Fig E2, *A*) or EBV-specific (Fig E2, *B*) $CD8^+$ T cells expressing granzymeA or granzyme K from healthy control subjects and patients with *PIK3CD* GOF mutations. Statistics were performed by using 2-way ANOVA (Fig E2, *A*) or a *t* test and Mann-Whitney test (Fig E2, *B*). **C** and **D,** Sorted T_{EM} or T_{EMRA} $CD8^+$ T cells were stimulated with anti-CD2, CD3, and CD28 mAbs. On day 5, cells were stimulated with PMA/ionomycin in the presence of Brefeldin A and monensin. Proportions of T_{EM}(Fig E2, *C*) or T_{EMRA} (Fig E2, *D*) cells expressing or secreting IFN-γ, IL-2, CD107a, granzyme B or perforin, or TNF was then determined. Statistics were determined by using a *t* test with the Mann-Whitney test. $*P < .05$ and $**P < .01$.

Figure E3

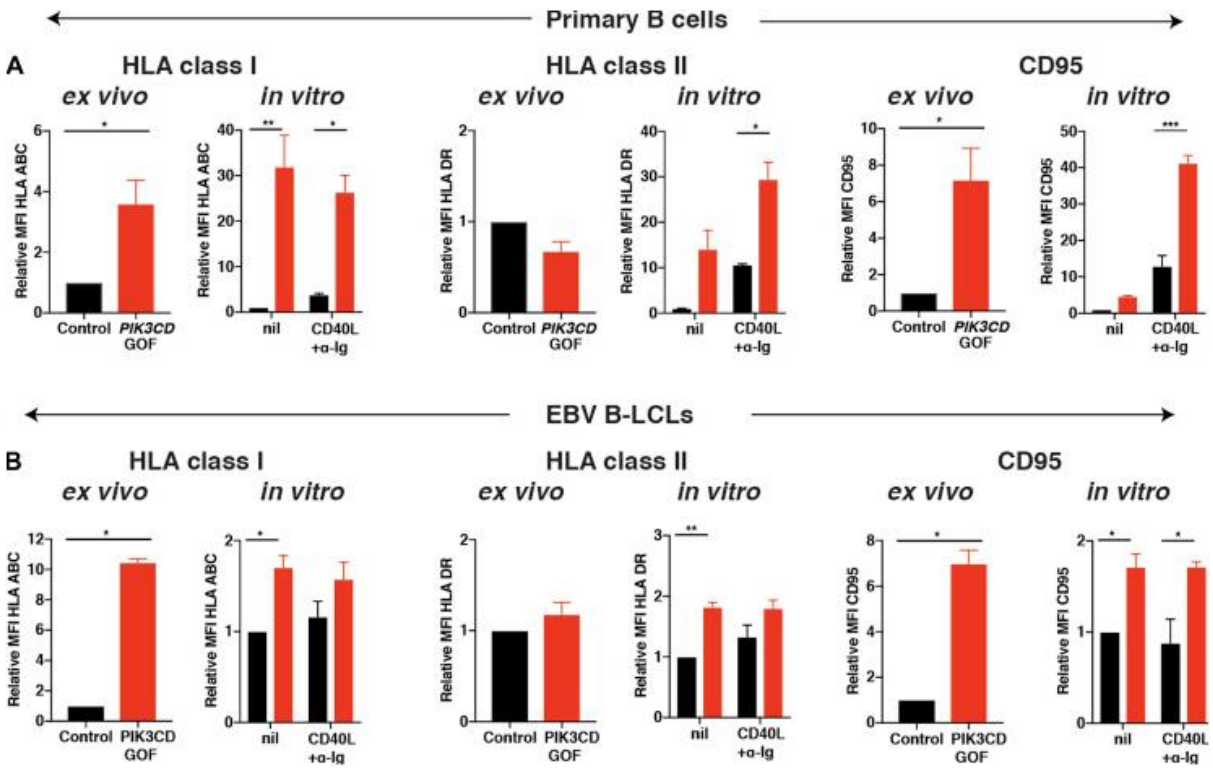

Expression of MHC and CD95 on primary B cells and LCLs in patients with *PIK3CD* GOF mutations. Peripheral blood B cells **(A)** or LCLs **(B)** were stained with mAbs to HLA class I (HLA-ABC), HLA class II (HLA-DR), or CD95 either *ex vivo* or after *in vitro* culture in the absence *(nil)* or presence of CD40L plus α-immunoglobulin. *Ex vivo* B cells were identified as $CD20^+$ cells. Expression of the indicated ligands was calculated relative to the mean fluorescence of control B cells or LCLs (normalized to 1.0). Statistics were performed by using a *t* test with the Mann-Whitney test or 2-way ANOVA. $*P < .05$, $**P < .01$, $***P < .001$, and $****P < .0001$.

Table 1

Demographic of subjexts given a diagnosis of PIL3CD GOF mutations

Family	Patients with *PIK3CD* GOF mutations	Mutation	Age (y)	Sex	Ethnicity	EBV	CMV	EBV (copies/μL)	Lymphoma	References
1	1	c.371G>A, p.G124D	40	F	White	+	−	850	No	23
2	2	c.1002C>A, p.N334K	12	F	AA	+	−	20,000	No	19
3	3	c.1573G>A p.E525K	67	F	White	+	−		EBV^+ DLBCL	Not published
	4	c.1573G>A p.E525K	37	M	White	+	+	1,850	No	19
	5	c.1573G>A p.E525K	14	M	White	+	+	<500	No	19
	6	c.1573G>A p.E525K	12	F	White	+	−		No	19
4	7	c.1573G>A p.E525K	7	F	Asian	+	−	8,050	No	19
5	8	c.1573G>A p.E525K	56	M	White	+	−		No	Not published
	9	c.1573G>A p.E525K	12	F	White	+	+	2,550	EBV^+ HL	19
	10	c.1573G>A p.E525K	23	M	White	+	−		No	Not published
6	11	c.3061G>A p.E1021K	12	M	AA/Hispanic	+	+	3,800	No	19
7	12	c.3061G>A p.E1021K	14	F	White	+	−	15,000	No	19
8	13	c.3061G>A p.E1021K	4.5	M	AA	+	+	1,600	No	Not published
9	14	c.3061G>A p.E1021K	14	F	White	+	−	4,250	MZBL	Not published
10	15	c.3061G>A p.E1021K	47	M	White	ND	ND		No	Not published
	16	c.3061G>A p.E1021K	14	F	White	ND	ND		No	Not published
	17	c.3061G>A p.E1021K	12	F	White	ND	ND		No	Not published
	18	c.3061G>A p.E1021K	7	F	White	ND	ND		No	Not published
11	19	c.3061G>A p.E1021K	23	M	White	−	−		DLBCL	Not published
12	20	c.3061G>A p.E1021K	20	F	White	ND	ND		No	Not published
13	21	c.3061G>A p.E1021K	23	M	White	−	−		No	Not published
14	22	c.3061G>A p.E1021K	16	M	Hispanic	−	−		No	Not published
15	23	c.3061G>A p.E1021K	5	M	White	−	−		No	Not published
16	24	c.3061G>A p.E1021K	15	F	European	−	−		No	31
17	25	c.3061G>A p.E1021K	13	M	White/Lebanese	−	−	ND	No	Not published
18	26	c.3061G>A p.E1021K	19	F	White	ND	ND		No	Not published
	27	c.3061G>A p.E1021K	46	F	White	ND	ND		No	Not published
19	28	c.3061G>A p.E1021K	25	F	Turkish	ND	ND		No	Not published
20	29	c.3061G>A p.E1021K	35	F	Turkish	ND	ND		No	19
21	30	c.3061G>A p.E1021K	29	F	White	+	−	450	No	Not published
22	31	c.3061G>A p.E1021K	7	F	White/Persian	−	−		No	Not published
	32	c.3061G>A p.E1021K	7	M	White/Persian	+	−		No	Not published
23	33	c.3061G>A p.E1021K	21	M	White	−	−		No	Not published
	34	c.3061G>A p.E1021K	14	M	White	−	−		No	Not published
24	35	c.3061G>A p.E1021K	10	M	White	−	−		No	Not published
25	36	c.3061G>A p.E1021K	10	M	White	ND	ND		No	Not published
26	37	c.3061G>A p.E1021K	16	F	Hispanic	+	−		No	Not published
27	38	c.3061G>A p.E1021K	9	F	Polynesian	+	+	ND	No	Not published
28	39	c.3074A>G p.E1025K	15	M	White	+	−	(Splenectomy)	No	24

Table E1

Peptide-MHC tetramers to identify EBV-sepecfic CD8* T cells

HLA type	Epitope sequence	Protein origin	Patients investigated
A∗0201	GLCTLVAML	BMLF-$1_{280-288}$	11, 12, 14, 15, 19, 20
A∗11∗	AVFDFKSDAK	EBNA-$3B_{246-253}$	7
B∗0702	RPPIFIRRL	EBNA-$3A_{247-255}$	3, 5, 6
B∗0801	FLRGRAYGL	EBNA-$3A_{325-333}$	2, 9
B∗0801	RAKFKQLL	BZLF-$1_{190-197}$	2, 9
B∗27	RRIYDLIEL	EBNA-$3C_{258-266}$	8

*Immudex Copenhagen Denmark

Table E2

mAbs used for lymphocyte pehotyping

Target	Fluorochrome	Clone	Supplier
CD3	BV786	UCHT1	BD Horizon
CD4	BUV395	SK3 (Leu3a)	BD Horizon
CD4	BUV737	SK3 (Leu3a)	BD Horizon
CD8	APC-Cy7	RPA-T8	BioLegend
CD8	BUV395	RPA-T8	BD Horizon
CD16	APC-Cy7	3G8	BioLegend
CD20	PB	2H7	BioLegend
CD38	FITC	HB7	eBioscience
CD45RA	PerCP-Cy5.5	HI100	eBioscience
CD45RA	BV605	HI100	BD Horizon
CD48	FITC	Tu145	BD PharMingen
CD56	BV605	HCD56	BioLegend
CD57	FITC	NK-1	BD PharMingen
CD70	APC	113-16	BioLegend
CD95	PE-CF594	DX2	BD Horizon
CD158a/g/h	PerCP-Cy5.5	HP-MA4	eBioscience
CD160	PE	BY55	BioLegend
CCR7	FITC	150503	R&D Systems
CCR7	PE Cy7	G043H7	BioLegend
2B4(CD244)	PE	eBioC1.7	eBioscience
Granzyme B	AF700	GB11	BD PharMingen
HLA ABC	APC–Fire 750	W6/32	BioLegend
HLA DR	PE-Cy7	G46-6	BD PharMingen
KLRG1	APC	REA261	Miltenyi Biotech
NKG2A (CD94)	PerCP-Cy5.5	DX22	BioLegend
NKG2D	PerCP-eFLuor710	1D11	eBioscience
NKp44	PE-Cy7	p44-8	BioLegend
PD-1	Biotin	eBioJ105	eBioscience
Perforin	PE-Cy7	B-D48	BioLegend
SA BV711	BV711		BD Horizon

AF, Alexa Fluor;
APC, allophycocyanin;
BV, Brilliant Violet;
FITC, fluorescein isothiocyanate;
PB, Pacific Blue;
PE, phycoerythrin;
PerCP, peridinin-chlorophyll-protein complex.

Table E3
mAbs used for muring lymphocyte phenotyping

Target	Fluorochrome	Clone	Supplier
CD3	PerCP-Cy5.5	17A2	BD Horizon
CD4	APC–eFluor 780	RM4-5	eBioscience
CD8	PB	53-6.7	BD Horizon
IFN-γ	PE-Cy7	XMG1.2	BD Horizon
TNF-α	PE	MP6-XT22	BioLegend
CD62L	APC	MEL-14	BD Horizon
CD62L	BV605	MEL-14	BioLegend
CD62L	FITC	MEL-14	eBioscience
CD44	FITC	IM7	BD Horizon
CD44	BV605	IM7	BD Horizon
CD45R/B220	FITC	RA3-6B2	BD Horizon
CD45R/B220	BV786	RA3-6B2	BD Horizon
CD25	PE	PC61	BD Horizon
CD25	APC	PC61	eBioscience

AF, Alexa Fluor;
APC, allophycocyanin;
BV, Brilliant Violet;
FITC, fluorescein isothiocyanate;
PB, Pacific Blue;
PE, phycoerythrin;
PerCP, peridinin-chlorophyll-protein complex.